Laboratory for Computational Proteomics

www.FenyoLab.org

E-mail: Info@FenyoLab.org

Facebook: *NYUMC Computational Proteomics Laboratory*

Twitter: *@CompProteomics*

Phosphotyrosine Signaling Networks in Epidermal Growth Factor Receptor Overexpressing Squamous Carcinoma Cells*[S]

April Thelemann‡, Filippo Petti‡, Graeme Griffin‡, Ken Iwata§, Tony Hunt¶, Tina Settinari‖, David Fenyo**‡‡, Neil Gibson‡, and John D. Haley‡§§

Overexpression and enhanced activation of the epidermal growth factor (EGF) receptor are frequent events in human cancers that correlate with poor prognosis. Anti-phosphotyrosine and anti-EGFr affinity chromatography, isotope-coded μLC-MS/MS, and immunoblot methods were combined to describe and measure signaling networks associated with EGF receptor activation and pharmacological inhibition. The squamous carcinoma cell line HN5, which overexpresses EGF receptor and displays sustained receptor kinase activation, was used as a model system, where pharmacological inhibition of EGF receptor kinase by erlotinib markedly reduced auto and substrate phosphorylation, Src family phosphorylation at EGFR Y845, while increasing total EGF receptor protein. Diverse sets of known and poorly described functional protein classes were unequivocally identified by affinity selection, comprising either proteins tyrosine phosphorylated or complexed therewith, predominantly through EGF receptor and Src family kinases, principally 1) immediate EGF receptor signaling complexes (18%); 2) complexes involved in adhesion and cell-cell contacts (34%); and 3) receptor internalization and degradation signals. Novel and known phosphorylation sites could be located despite the complexity of the peptide mixtures. In addition to interactions with multiple signaling adaptors Grb2, SHC, SCK, and NSP2, EGF receptors in HN5 cells were shown to form direct or indirect physical interactions with additional kinases including ACK1, focal adhesion kinase (FAK), Pyk2, Yes, EphA2, and EphB4. Pharmacological inhibition of EGF receptor kinase activity by erlotinib resulted in reduced phosphorylation of downstream signaling, for example through Cbl/Cbl-B, phospholipase Cγ (PLCγ), Erk1/2, PI-3 kinase, and STAT3/5. Focal adhesion proteins, FAK, Pyk2, paxillin, ARF/GIT1, and plakophillin were down-regulated by transient EGF stimulation suggesting a complex balance between growth factor induced kinase and phosphatase activities in the control of cell adhesion complexes. The functional interactions between IGF-1 receptor, lysophosphatidic acid (LPA) signaling, and EGF receptor were observed, both direct and/or indirectly on phospho-Akt, phospho-Erk1/2, and phospho-ribosomal S6. *Molecular & Cellular Proteomics 4: 356–376, 2005.*

Overexpression and enhanced activation of the epidermal growth factor (EGF)[1] receptor are frequently observed in human cancers (1, 2), and abnormal activation of the receptor's intrinsic tyrosine phosphotransferase activity correlates with poor prognosis (3). Overexpression of EGF receptor is a common event in tumors of the breast, bladder, lung, head and neck, and central nervous system. Inhibitors of EGF receptor function have shown clinical utility, and the definition of key EGF receptor signaling pathways has become increasingly important in understanding the consequences of drug action (2). The EGF receptor family of receptor tyrosine kinases, EGFR, ErbB2, ErbB3, and ErbB4, can heterodimerize to allow a diversity of ligand responses with accompanying changes in the rates and routes of internalization and degradation (4). The EGF receptor is a membrane glycoprotein having an external cysteine-rich ligand binding domain, linked by a short single transmembrane sequence to intracellular tyrosine kinase and carboxyl-terminal scaffolding domains (5, 6). The binding of ligands including EGF, TGFα, amphiregulin, and HB-EGF results in an activation of the receptor tyrosine kinase activity and autophosphorylation at multiple tyrosine residues located in the C-terminal domain (1). When phosphorylated, the C-terminal domain serves as a scaffold for the binding of Src homology 2 (SH2)- and phosphotyrosine binding (PTB)-containing adaptor proteins, for example Grb2, Shc, NSP1, and NSP2, which can transduce mitogenic and cell survival sig-

From ‡OSI Pharmaceuticals, Inc., Farmingdale, NY 11735 and §Wilderness Drive, Boulder, CO 80301; ¶Applied Biosystems, Inc., Framingham, MA 01701 and ‖Foster City, CA 94404; and **Proteometrics, New York, NY 10018

Received, September 2, 2004, and in revised form, January 15, 2005

Published, MCP Papers in Press, January 17, 2005, DOI 10.1074/mcp.M400118-MCP200

[1] The abbreviations used are: EGF, epidermal growth factor; HNSCC, head and neck squamous carcinoma; EGFR, epidermal growth factor receptor; IGF-1, insulin-like growth factor-1; FAK, focal adhesion kinase; HB-EGF, heparin-binding epidermal growth factor; SH2, Src homology 2 domain; PTB, phosphotyrosine binding domain; LPA, lysophosphatidic acid; TGFα, transforming growth factor α; IC_{50}, half maximal inhibitory concentration; pY, phosphotyrosine; SCX, strong cation exchange; PLCγ, phospholipase Cγ; PI3-kinase, phosphatidyl inositol-3 kinase; GO, Gene Ontology database; OSI-774, erlotinib (Tarceva).

nals. Substrate binding in turn can stimulate additional protein-protein interactions to assemble competent signaling complexes required to coordinate the diverse responses elicited by ligand binding (7), and the tyrosine phosphorylation of transiently interacting substrates can establish scaffolds for SH2 and PTB complex formation at distant sites. The compartmentalization of EGF receptors also has marked effects on the repertoire of substrates and interacting factors through which receptor signaling is achieved. For example EGF receptors have been shown to cluster in caveolae (8) where autophosphorylation results in interactions with phospholipid and calcium-dependent substrates enriched within this lipid-raft-like microenvironment. Similarly the translocation and internalization of the receptor into early endosomes place the receptor in an important subcellular localization for the transduction of signals through the Ras-Raf-Mek-Erk pathway important in the mitogenic effects of EGF (8). Thus both EGF receptor protein interactions as well as the cellular location of receptor complexes determine the downstream signals produced.

In vitro and clinical studies have shown considerable variability between cell lines and tumors in their cellular responses to EGF receptor inhibition, which in part has been shown to derive from EGF receptor-independent activation of the phosphatidyl inositol 3-kinase (PI3-kinase) pathway, leading to the continued phosphorylation of the anti-apoptotic serine-threonine kinase Akt (9). The molecular determinants to alternative routes of PI3-kinase activation and consequent EGF receptor inhibitor insensitivity are an active area of investigation (10). For example the insulin-like growth factor-1 receptor (IGF-1 receptor), which strongly activates the PI3-kinase pathway, has been implicated in cellular resistance to EGF inhibitors. The roles of other tyrosine kinases in mediating insensitivity to selective EGF receptor inhibition are less clear, for example those of the Src family, which participate in the mitogenic and survival signals generated by lysophosphatidic acid (LPA). Similarly cell-cell and cell adhesion networks can also exert survival signals through the PI3-kinase pathway (11) and would be postulated to impact cell sensitivity to EGF receptor blockade. The ability of tumor cells to maintain growth and survival signals in the absence of adhesion to extracellular matrix or cell-cell contacts is important not only in the context of cell migration and metastasis but also in maintaining cell proliferation and survival in changing tumor environments where extracellular matrix is being remodeled and cell contact inhibition is abrogated. The EGF receptor and proteins controlling cell adhesion assembly and disassembly have been shown to physically interact and cross-regulate in a complex manner dependent on receptor activity and cell adhesion factors (12, 13).

The principle aim of this study was to 1) better define EGF receptor signaling networks within tumor cells abnormally overexpressing EGF receptors and 2) define those signaling proteins and pathways most sensitive to inhibition of EGF receptor kinase activity. The squamous carcinoma cell line HN5 (14) was used as a model system to investigate phosphotyrosine-dependent cellular signaling. HN5 cells show a high basal level of EGF receptor activity, derived in part from autocrine production of TGFα, and are sensitive to EGF receptor inhibition. Receptor overexpression is prevalent in squamous cell carcinomas of the head and neck (HNSCC), occurring in over 40% of cases, and inhibition of EGF receptor signaling has been shown to reduce tumor xenograft growth *in vivo* (15). Erlotinib, a selective EGF receptor kinase inhibitor, has an IC_{50} for cellular EGF receptor kinase inhibition of ~50 nM. The inhibition of HN5 cell proliferation is closely correlated to EGF receptor inhibition, with an IC_{50} of 90 nM. Here anti-phosphotyrosine (anti-pY) and anti-EGF receptor affinity chromatography were coupled with multiple MS approaches (Fig. 1) to define proteins and protein complexes associated with EGF receptor signaling and with kinase inhibition. In addition to interactions with multiple signaling adaptors Grb2, SHC, SCK, and NSP2, EGF receptors in HN5 cells were shown to form direct or indirect physical interactions with additional kinases including ACK1, focal adhesion kinase (FAK), Pyk2, Yes, EphA2, and EphB4. Models of EGF receptor signaling in HNSCC were constructed. The relative abundance of anti-pY-selected proteins after EGF receptor kinase inhibition by erlotinib (OSI-774 *Tarceva*; Ref. 16) and after hyperstimulation of EGF receptor kinase activity by addition of exogenous EGF was measured by protein immunoblot and peptide ICAT methods (17). Pharmacological inhibition of EGF receptor ki-

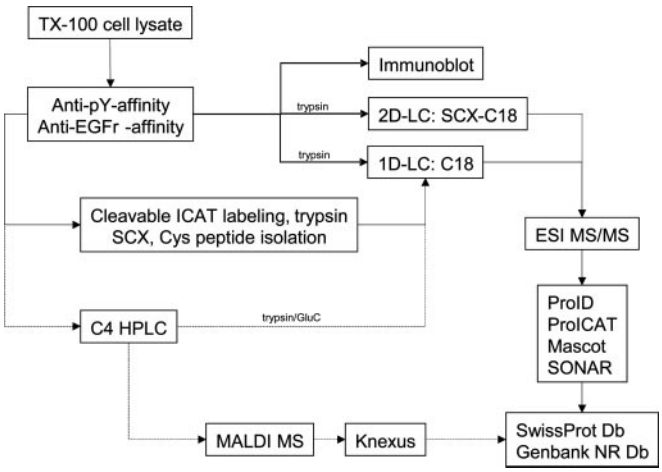

FIG. 1. **Experimental schema used for protein and peptide fractionation, identification, and measurement.** HN5 cell detergent lysates were prepared using Triton X-100 (TX-100) containing buffer followed by anti-pY or anti-EGFR affinity selection. Protein digests were fractionated by one- or two-dimensional LC (1D-LC or 2D-LC) followed by MS, either ESI or MALDI. Proteins were identified by peptide MS or MS/MS spectra using multiple software tools (ProID, ProICAT, Mascot, SONAR, and Knexus). In quantitation experiments, proteins were labeled with ICAT reagents prior to proteolytic digestion with trypsin and SCX chromatography. In MALDI-MS experiments, proteins were fractionated by C4 reverse-phase HPLC prior to proteolytic digestion (either trypsin or GluC) and MS.

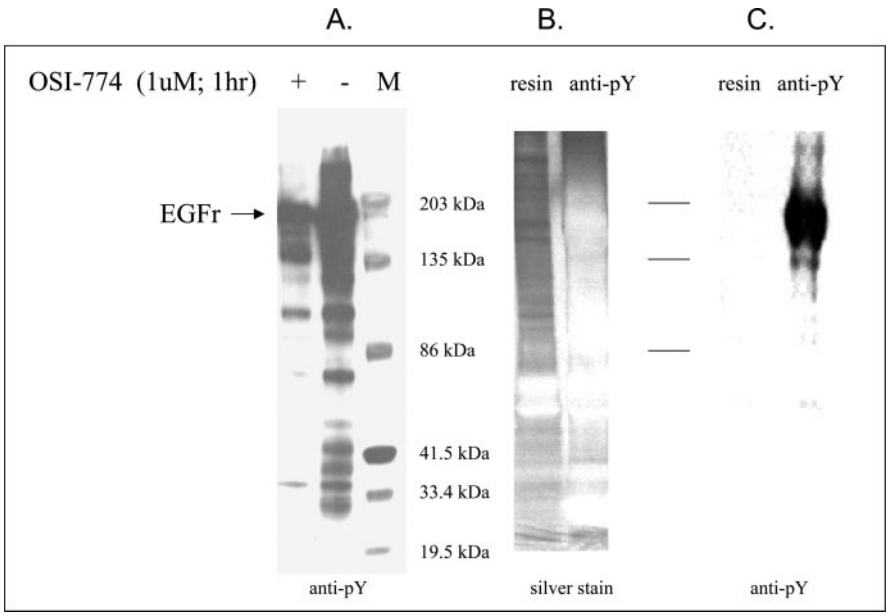

FIG. 2. *A*, HN5 cell phosphotyrosine containing proteins obtained by anti-pY affinity selection were subjected to anti-pY immunoblot, overexposed to reveal substrate phosphorylation. Lysates were prepared from cells with or without blockade of EGF receptor by erlotinib (OSI-774) for 60 min followed by EGF stimulation (10 ng/ml) for 10 min. *B*, silver-stained protein fractions from anti-pY affinity and control resin affinity steps, overexposed to reveal low background binding in the resin control. *C*, anti-pY immunoblot of proteins isolated on control resin and anti-pY immunoaffinity resin showing low background binding of tyrosine-phosphorylated proteins to the resin control.

nase activity by erlotinib resulted in reduced phosphorylation of downstream signaling, for example through Cbl/Cbl-B, phospholipase Cγ (PLCγ), Erk1/2, PI-3 kinase, and STAT3/5. Focal adhesion proteins, FAK, Pyk2, paxillin, ARF/GIT1, and plakophillin were down-regulated by transient EGF stimulation, suggesting a complex balance between growth factor-induced kinase and phosphatase activities in the control of cell adhesion complexes. The functional interactions between IGF-1 receptor, LPA signaling, and EGF receptor were observed, both direct and/or indirectly on phospho-Akt, phospho-Erk1/2, and phospho-ribosomal S6.

EXPERIMENTAL PROCEDURES

Preparation of Immobilized Antibody Affinity Resins—Immunoaffinity resins (anti-pY and anti-EGF receptor) were prepared by covalent coupling to resin followed by low pH washing to remove noncovalently bound antibody, a potential source of significant immunoglobulin heavy and light chain contamination in later steps. Freshly prepared immunoaffinity resins were used for each biological experiment to maximize binding and reduce carryover. Anti-pY antibodies PY20 (Exalpha Biologicals, Inc., Watertown, MA) and PY100 (Cell Signaling Technology, Beverly, MA) were mixed in an 8:1 ratio and bound to Protein G-resin (Pierce, Rockford, IL) for 30 min at room temperature. In separate experiments, anti-EGF receptor antibody, recognizing an extracellular epitope (EGFR.1, Ref. 18; BD Bioscience, San Diego, CA), was similarly immobilized. Antibody resins were washed extensively, and 0.02 M dimethylpimelidate dihydrochloride (DMP, in 0.2 M triethanolamine, pH 8.2; Pierce) was added and mixed for 1 h on a rotating platform. Crosslinking was terminated by washing with three resin volumes of 0.2 M triethanolamine, pH 8.2, once with 0.2 M sodium citrate, pH 2.8 (to remove noncovalently bound IgG), and finally with three volumes of 10 mM TrisHCl, pH 8.2. Antibody crosslinked resins were stored at 4 °C until use. In later experiments disuccinimidyl suberate (DSS) crosslinker was substituted for DMP (Pierce) with similar results.

Preparation of HN5 Cell Lysate, Anti-pY, and Anti-EGF Receptor Affinity Chromatography and Protein Immunodetection—Approximately 2×10^8 HN5 cells (14) were grown in Dulbecco's modified Eagle's medium with 10% fetal bovine serum. HN5 cell extracts were prepared by mild detergent lysis (1% Triton X-100) containing protease and phosphatase inhibitors (see below) to enhance the preservation of protein interactions, lost when deoxycholate-containing lysis buffers (*e.g.* RIPA) were used. The selective EGF receptor kinase inhibitor erlotinib (1 μM OSI-774) was added to HN5 cells for 60 or 120 min prior to lysis. EGF-treated cells were incubated with ligand (10 ng/ml) for 10 min prior to lysis unless otherwise stated. Cells were washed once with PBS prior to lysis in 50 mM HEPES, pH 7.5, 150 mM NaCl, 1.5 mM $MgCl_2$, 1 mM EGTA, 10% glycerol, 1% Triton X-100, 1 mM 4-(2-aminoethyl)benzenesulfonyl fluoride hydrochloride, 0.8 μM aprotinin, 20 μM leupeptin, 40 μM beestatin, 15 μM pepstatin A, 14 μM E-64 [1:100 dilution of protease inhibitor mixture P8340; Sigma, St. Louis, MO], sodium orthovanadate, sodium molybdate, sodium tartrate, and imidazole [1:100 dilution of phosphatase inhibitor mixture P5726; Sigma] for ~3 min. Insoluable material was removed by centrifugation (13,000 $\times$ *g*, 10 min, 4 °C). Protein concentration was determined by microBCA assay (Pierce). Lysates were precleared by incubation with blank Protein-G resin for 30 min at 4 °C prior to immunoprecipitation to reduce nonspecific binding. Antibody resins were equilibrated with lysis buffer and incubated with HN5 cell lysates for 2–4 h at 4 °C with rotation. Antibody-antigen complexes were washed with >200 volumes of 10 mM TrisHCl, pH 8.0, 150 mM NaCl at 4 °C, proteins eluted with 0.1% TFA, 5% methanol, and dried *in vacuo*. The initial anti-pY affinity step yielded ~50–100 μg of protein from 2×10^8 cells, representing an approximate 1,000-fold enrichment, greatly reducing sample complexity for subsequent LC-MS/MS protein identification. Visual inspection of SDS-PAGE-fractioned anti-pY affinity-isolated proteins (Fig. 2*A*) or nonspecific proteins trapped on resin control (Fig. 2, *B* and *C*) or goat anti-rabbit antibody control (data not shown) qualitatively indicated minimal nonspecific binding and generally low IgG release from the resin. Equivalent amounts of protein extract, as determined by BCA assay, were subject to SDS-PAGE. Protein immunodetection was performed by electrophoretic transfer of SDS-PAGE-separated proteins to nitrocellulose, incubation with antibody, and chemiluminescent second step detection (ECL; Amersham, Piscataway, NJ).

Antibodies included: p130 Cas (#sc-860; Santa Cruz Biotechnology, Santa Cruz, CA), phospho-Shc (#2434; Cell Signaling, Beverly, MA), phospho-Paxillin (#2541; Cell Signaling), phospho-Akt (#9271;

Cell Signaling), phospho-HER2/ErbB2 (#2245; Cell Signaling), phospho-p44/42 MAP kinase (#9101; Cell Signaling), phospho-EGFR (Tyr^{845}) (#2231; Cell Signaling), phospho-EGFR (Tyr^{992}) (#2235; Cell Signaling), phospho-EGFR (Tyr^{1045}) (#2237; Cell Signaling), EGFR (#2232; Cell Signaling), Pyk2 (#06–559-MN; Upstate Biotechnology, Lake Placid, NY), phospho-Caveolin-1 (#3251; Cell Signaling), phospho-p70 S6 kinase (#9205; Cell Signaling), phospho-GSK-3α/β (#9331; Cell Signaling), phospho-EGFR (Tyr^{1068}) (#2236; Cell Signaling), phospho-Src family (Tyr^{416}) (#2101; Cell Signaling), phospho-Src (Tyr^{527}) (#2105; Cell Signaling), FAK (#06–543-MN; Upstate Biotechnology), Karyopherin B1 (#sc-11367; Santa Cruz Biotechnology), 14-3-3ζ (#sc-1019; Santa Cruz Biotechnology), 14-3-3ϵ (#610542; BD Transduction Laboratories, San Jose, CA), ACK (#sc-323; Santa Cruz Biotechnology), α-catenin (#sc-9988; Santa Cruz Biotechnology), Plakophilin 2 (#610788; BD Transduction Laboratories), GRB2 (#3972; Cell Signaling), δ-catenin (#07-259; Upstate Biotechnology), EF-1α (#05-235; Upstate Biotechnology), Tyk 2 (#sc-169; Santa Cruz Biotechnology), γ-catenin (#sc-8415; Santa Cruz Biotechnology), EphA2 receptor (#34-7400; Zymed Laboratories, South San Francisco, CA), clathrin heavy chain (#CP45; Oncogene Research Products, Boston, MA), c-Yes (#06-514; Upstate Biotechnology), and IGF-1R-β chain (#sc-713; Santa Cruz Biotechnology).

Peptide Identification by LC-MS/MS Fragment Ion Spectra Database Searching—Proteins isolated by anti-pY affinity chromatography were denatured, reduced, carboxamidomethylated, and proteolytically cleaved with trypsin. Peptides were introduced into the Q-TOF mass spectrometer either using reverse phase (C18) HPLC or, to further reduce sample complexity and ion suppression, using coupled strong cation exchange-reverse phase (SCX-C18) HPLC. The use of multiple overlapping methods (Fig. 1) greatly improved the breadth of protein identification and peptide coverage, with greatest coverage with cleavable-ICAT and SCX-C18 strategies (data not shown). Two-dimensional SCX-C18 chromatography (19) was performed using a 1 × 5-mm cation exchange column packed with polysulfoethyl A resin (SCX; PolyLC, Columbia, MD) and 0.32 × 150-mm column packed with Pepmap C18 resin (LC Packings, San Francisco, CA) loaded and developed at 30 μl/min. Peptides were detected by UV absorbance at 214 nm using a 250-nl internal volume flow cell with a 2-mm path length. Peptides were eluted from the C18 resin then coupled directly to the mass spectrometer, at a flow rate of ~2 μl/min. One-dimensional C18 chromatography was performed using a 0.1 × 150-mm column packed with C18 resins (MagicC18, Michrom Bioresources, Auburn, CA or Vydac MS218, Nest Group, Southborough, MA) and developed using a 2–70% ACN, 0.1% formic acid gradient with a flow rate of ~500 nl/min. The electrospray source was fitted with an uncoated tapered fused silica tip (10–15-μm inner diameter; New Objective, Cambridge, MA) to which a voltage of 3.0 kV was applied with nebulizing nitrogen gas. Information-dependent MS and MS/MS acquisitions were made on an orthogonal Q-TOF (qQ-TOF) instrument (Sciex, Toronto, Canada) using a 1-s survey scan (*m/z* 400–1,200) followed by three consecutive 3-s product ion scans of 2^+, 3^+, and 4^+ parent ions with a 4-min exclusion period. The product ion mass range was typically limited to 60–1,000 Da scanned in two cycles or 60–1,600 Da scanned in three cycles, and where collision energy was dynamically ramped according to mass and charge state, were used to maximize the duty cycle of the instrument. In later experiments, ions were stored in the second quadrapole and released in synchrony with the pulsing of ions in TOF detector, resulting in an ~ 5–8-fold increase in sensitivity. Data were acquired using Sciex Analyst QS software. Proteins were identified from survey and product ion spectral data, with an MS and MS/MS mass tolerance of 0.15 Da, using both Swiss-Prot and Genbank NR databases and ProID (Version 1.0 EP2; Applied Biosystems, Foster City, CA), Mascot (Matrix Science, London, United Kingdom), and SONAR (Proteometrics, New York, NY) search programs. Mascot and SONAR searches accessed merged dta format files. Sciex wiff files were converted to dta format ("Export IDA Spectra" script) and merged using the Merge function from Matrix Science. Protein sequences for porcine trypsin, mouse immunoglobulin constant regions, and variable regions from the anti-pY antibody PY20 were appended to the human Swiss-Prot database. One missed tryptic cleavage was allowed and post-translational modifications considered included only cysteine derivitization and tyrosine phosphorylation. ProID confidence scores of >90% were considered, after which spectra were manually inspected as no criteria were found for any of the search programs that would allow correct unattended protein assignments without an unacceptably high false-negative rate. Mascot scores of >20 and SONAR expectation values of <1 were considered. Only proteins assigned with two or more peptides were included in Table I. Peptide redundancy was prevented by manually sorting the peptide lists in Excel.

The cleavable-ICAT labeling method was used to differentially measure protein abundance between two biological states, for example after EGF receptor blockade with erlotinib or after stimulation of receptor activity with EGF. After anti-pY affinity selection (described above), samples were dried *in vacuo*, denatured, and cysteine residues derivitized with either light isotope ICAT label (control group) or heavy isotope ICAT label (treatment group) according to the manufacturer's protocol (Appled Biosystems, Foster City, CA) and subjected to information-dependent LC-MSMS as described above. The ratio between heavy and light labeled peptide provides a relative measure to the differential protein abundance within the anti-pY affinity fraction. ICAT-labeled proteins were identified using ProICAT (Version 1.0 SP3; Applied Biosystems), Mascot and SONAR, while the relative quantification of ICAT ion pairs was determined using ProICAT. ProICAT confidence scores of >90% were considered, after which spectra were inspected manually to confirm peptide sequence assignments. Multiple bioinformatics tools were used to visualize and analyze the connections between proteins and complexes identified by anti-pY affinity selection and LC-MS/MS spectra searching. Tools included Network Explorer (www.ingenuity.com) and ScanSite (scansite.mit.edu).

Protein Fractionation and Comparative MALDI-MS Peptide Mapping of Trypsin and gluC Digests—Anti-pY affinity fractions were reduced (100 mM DTT) and carbamidomethylated (50 mM iodoacetamide, 1 h, room temperature, in the dark). Samples were fractionated by capillary C4 reverse-phase LC (0.32 mm × 150 mm) using a 5–90% gradient of increasing ACN, 0.1% TFA over 90 min with a flow rate of 3 μl/min. Reverse-phase protein fractions (~5–20%, 20–30%, 30–40%, 40–50%, 50–60%, and 60–90% ACN) were reduced in volume and digested in 50 mM NH_4CO_3, 5% ACN with 50 μg/ml trypsin or 50 μg/ml gluC for 18 h at 37° C. Samples were desalted using micro reverse-phase C18 tips (Millipore Corp., Billerica, MA) and eluted in 50% ACN-water. Peptide masses were determined by MALDI (DE-Pro; Applied BioSystems, Framingham, MA) in reflector mode (2-m flight length) with a positive ion accelerating voltage of 20 kV, a grid voltage of 12.8 kV, guide wire voltage of 1,400 V, using 120 ns delayed extraction. Recrystallized α-cyano-4-hydroxycinnamic acid (4-HCCA) and dihydrobenzoic acid (DHB) were used as matrices, generally using dried droplet methods. Greater than 200 scans were averaged per spectra. Trypsin and gluC autodigestion products were used as internal mass standards. Protein prediction based on peptide mass information was performed by interrogation of the Swiss-Prot database using the Knexus search program (Proteometrics), searched at a resolution of 30 ppm for proteins from 10 to 300 kDa. Post-translational modifications considered included only cysteine modifications and phosphorylation of tyrosine residues.

TABLE I

Proteins and protein classes isolated by anti-pY affinity chromatography from HN5 HNSCC cells

Accession numbers from Swiss-Prot and GenBank, protein names, the number of distinct peptides identified by LC-MS/MS, and the mean percent confidence and score for peptides comprising the identified protein. Key domains are listed. Proteins detected by immunoblot are indicated by bolded accession numbers. Proteins identified by anti-EGFr affinity chromatography are indicated by italic protein names. Proteins uniquely identified by SONAR are indicated by "s."

Accession ID	Protein class and name	Unique peptides	Mean % confidence	Mean % score	Select domains
	Calcium regulation				
gi|7656952	Calcyclin binding protein	4	99	18	SGS, p23
sp|Q14257	Reticulocalbin 2 precursor (Calcium-binding protein ERC-55)	3	99	30	EF-hand, ER_TARGET 1
sp|P31949	*S100 calcium-binding protein A11 (Calgizzarin)*	2	99	28	CaBP_S100, EF-hand
gi|4506773	S100 calcium-binding protein A9 (Calgranulin B)	2	99	26	CaBP_S100, EF-hand
sp|P16615	*Sarcoplasmic/endoplasmic reticulum calcium ATPase 2*	2	99	25	Calcium_ATPase, Hydrolase
	Cell cycle				
gi|4758046	*Cell cycle progression 2 protein*	2	99	14	FAST_Lau_rich
sp|P06493	*Cell division control protein 2 homolog (p34 protein)*	4	99	29	Ser_thr_pkin_AS, Ser_thr_pkinase
	Cell proliferation, survival				
sp|P42655	*14-3-3 protein ϵ (Mitochondrial import stimulation)*	3	99	26	14-3-3
sp|P31947	*14-3-3 protein σ (Stratifin) (Epithelial cell marker protein 1)*	4	99	22	14-3-3
sp|P27348	*14-3-3 protein τ*	4	99	26	14-3-3
sp|P29312	*14-3-3 protein ζ (PKC inhibitor protein-1)*	4	99	28	14-3-3
sp|P35222	Catenin β (88kDa)	2	92	19	Armadillo
sp|P00533	*Epidermal growth factor receptor precursor*	85	99	35	Furin-like, Tyr_pkinase
sp|P09382	Galectin-1 (Beta-galactoside-binding lectin L-14-I)	2	99	22	Galectin, Gal-bind_lectin 1
sp|P29354	*Growth factor receptor-bound protein 2 (GRB2 adapter protein)*	4	98	27	Neu_cyt_fact_2, SH2, SH3
sp|P04792	*Heat shock 27 kDa protein (Stress-responsive protein 27)*	10	99	39	Crystallin_alpha, Hsp20
sp|P08069	Insulin-like growth factor I receptor precursor	2	99	23	FN_III, Furin-like 1, Tyr_pkinase
sp|Q14192	*LIM-protein 3 (SLIM 3) (LIM-domain protein DRAL)*	3	98	20	LIM domain
sp|Q16539	Mitogen-activated protein kinase 14	2	99	29	p38_MAPK, Ser_thr_pkinase
sp|P27361	Mitogen-activated protein kinase 3 (and/or MAPK1; Erk 1,2)	2	99	23	MAPK, Ser_thr_pkinase
sp|P29597	Non-receptor tyrosine-protein kinase TYK2	2	99	24	FERM, Tyr_pkinase, SH2
gi|4885525	NSP1; SH2 domain containing 3A; novel SH2-containing protein 1	4	99	26	SH2, GEF for Ras-like small GTPases
gi|4502371	*NSP2, breast cancer antiestrogen resistance 3*	11	99	30	SH2, GEF for Ras-like small GTPases
sp|P19174	PLCγ1; 1-phosphatidylinositol-4,5-bisphosphate phosphodiesterase γ	3	99	23	C2, EF-hand, PH, PI_PLC, SH2, SH3
sp|O75340	Programmed cell death protein 6	2	99	38	EF-hand
sp|P07947	*Proto-oncogene tyrosine-protein kinase YES (p61-YES)*	7	99	33	Prot_kinase, SH2, SH3, Tyr_pkinase
sp|P04626	*Receptor protein-tyrosine kinase erbB-2 precursor*	7	99	32	Furin-like, Tyr_pkinase, YLP_motif
sp|P29353	*SHC transforming protein*	6	99	29	PID_domain, PTB_PID, SH2
sp|P40763	*Signal transducer and activator of transcription 3 (STAT3)*	8	98	25	P53-like, SH2, STAT
sp|P12931	Src proto-oncogene tyrosine-protein kinase	6	99	28	SH2, SH3, Tyr_pkinase, Tyr_pkinase_AS
	Cell adhesion, cytoskeleton				
gi|8922075	*ACK1, activated p21cdc42Hs kinase*	4	97	23	SH3, Tyr_pkinase, UBA_domain
sp|P02570	Actin, cytoplasmic 1 (and/or α, γ)	6	99	37	Actin, Actin_like
sp|O43707	α-actinin 4 (F-actin cross linking; also α-actinin-1)	4	99	18	Actbind_actnin, Calponin-like, Spectrin, EF-hand
sp|P04083	Annexin I (lipocortin I; chromobindin 9) (P35)	2	99	25	Annexin
sp|P07355	Annexin II (lipocortin II; chromobindin 8)	2	99	36	Annexin
sp|P08758	Annexin V (lipocortin V; endonexin II; calphobindin I)	3	99	24	Annexin
sp|Q14161	ARF GTPase-activating protein GIT1	2	99	18	ANK, GIT, hRIP_like

TABLE I—*continued*

Accession ID	Protein class and name	Unique peptides	Mean % confidence	Mean % score	Select domains
trm|Q99018	BPAG2, 180-kDa bullous pemphigoid antigen-2	2	98	15	Collagen
sp|P35221	*Catenin α-1 (Cadherin-associated protein) (α E-catenin)*	10	99	28	Alpha_catenin, Vinculin
sp|O60716	*Catenin Δ-1 (p120 catenin; cadherin-associated src)*	9	99	32	Armadillo
sp|Q03135	*Caveolin-1*	2	99	44	Caveolin
sp|P56945	*CRK-associated substrate (p130Cas)*	16	99	37	SH3
gi|30410805	*CUB domain-containing protein 1 isoform 1 (SIMA 135/CDCP1)*	7	97	21	CUB domain
gi|17975768	Ephrin receptor EphB3 precursor; EPH-like tyrosine kinase-2	3	97	29	Tyrosine kinase, TNFR domain, FN_III
sp|P29317	*Ephrin type-A receptor 2 precursor*	7	99	27	FN_III, SAM, Tyr_pkinase
sp|P54760	*Ephrin type-B receptor 4 precursor*	2	99	29	FN_III-like, Gal_bind_like, SAM, Tyr_pkinase
sp|P98172	*Ephrin-B1 precursor (EPH-related receptor tyrosine kinase ligand 2)*	2	99	25	Cupredoxin, Ephrin
sp|Q05397	*Focal adhesion kinase 1 (FADK 1) (pp125FAK, PTK2)*	19	99	31	Band_4, Focal_AT, Tyr_pkinase
sp|Q12931	Heat shock protein 75 kDa (HSP75; TRAP-1)	2	99	28	ATPbind_ATPase, Hsp90
sp|P16144	Integrin β-4 precursor (GP150) (CD104 antigen)	3	99	26	Calx_beta, FN_III, Integrin_B, Plexin-like, VWF_A
sp|P23229	Integrin α-6 precursor (VLA-6) (CD49f)	3	98	28	Integrin_alpha
sp|P14923	Junction plakoglobin (Desmoplakin III; gamma catenin)	2	99	24	Armadillo
sp|P13645	Keratin, type I cytoskeletal 10	4	99	29	IF, Keratin_I
sp|P02533	*Keratin, type I cytoskeletal 14*	6	99	39	IF, Keratin_I
sp|Q04695	*Keratin, type I cytoskeletal 17*	3	99	35	IF, Keratin_I
sp|P04264	*Keratin, type II cytoskeletal 1*	3	99	25	IF, keratin_II
sp|P13647	*Keratin, type II cytoskeletal 5*	6	99	26	IF, Keratin_II
sp|P02538	*Keratin, type II cytoskeletal 6A*	5	99	32	IF, Keratin_II
sp|P49023	*Paxillin*	11	99	33	Paxillin, LIM_DOMAIN_1, LIM_DOMAIN_2
sp|Q99959	*Plakophilin 2*	2	99	24	Armadillo
sp|Q99569	Plakophilin 4 (p0071)	2	98	24	Armadillo
sp|Q15149	Plectin 1 (PLTN) (PCN) (Hemidesmosomal protein 1)	26	99	33	Actbind_actnin, Calponin-like, Plectin, Spectrin
gi|4758414	Polypeptide *N*-acetylgalactosaminyltransferase 3	2	99	29	—
gi|16877878	*PRO1855 protein (leucine-rich domain; similar to flightless-1)*	5	s		Leucine-rich repeat (LRR) protein
sp|Q14289	*Protein tyrosine kinase 2 β (Focal adhesion kinase 2)*	3	99	27	Band_4, Focal_AT, Tyr_pkinase
sp|Q13671	Ras and Rab interactor 1 (RIN1)	2	99	39	RA_domain, SH2, VPS9
sp|Q14155	Rho GEF-7 (PAK-interacting exchange protein)	3	99	23	GDS_CDC24, PH, RhoGEF, SH3
sp|Q14247	Src substrate cortactin (Amplaxin) (Oncogene EMS1)	2	99	23	Hs1/Cortactin, Neu_cyt_fact_2, SH3
sp|P10599	*Thioredoxin (ATL-derived factor)*	2	98	27	Thiored, Thioredox_dom2
sp|P05209	*Tubulin α-1 chain*	13	99	29	Tubulin_FtsZ
sp|P05218	*Tubulin β-5 chain*	18	99	29	Beta_tubulin, Tub_FtsZ_C, Tubulin_FtsZ
sp|P52735	Vav-2 protein	3	94	17	DAG_PE-bind, GDS_CDC24, PH, RhoGEF, SH2, SH3
	Nuclear transport				
sp|O43592	*Exportin T (tRNA exportin)*	2	99	29	ARM, Exportin-t
sp|Q14974	*Importin β-1 subunit (Karyopherin β-1 subunit)*	8	99	30	Armadillo, HEAT_repeat, Importinb_N
sp|O00410	Importin β-3 subunit (Karyopherin β-3 subunit)	5	99	23	HEAT_repeat, Importinb_N
sp|P55060	*Importin-α re-exporter (Chromosome segregation 1-like)*	4	99	29	CAS_CSE1, Importinb_N
gi|5453998	RAN binding protein 7; RAN binding protein 7; importin 7	2	99	28	Importinb_N, ARM repeat
sp|P55072	Transitional endoplasmic reticulum ATPase (TER ATPase)	3	99	23	AAA_ATPase, AAA_CDC48

TABLE I—*continued*

Accession ID	Protein class and name	Unique peptides	Mean % confidence	Mean % score	Select domains
	RNA maturation, protein biosynthesis				
sp|P17075	40S ribosomal protein S20	2	98	9	Ribosomal_S10, Ribosomal_S10s/a
sp|P46782	40S ribosomal protein S5	2	99	21	Ribosomal_S7, Ribosomal_S7s/a
sp|O00571	DEAD-box protein 3 (Helicase-like protein 2) (HLP2)	2	98	24	DEAD_box, DEAD_ATP_HELICASE
sp|P04720	*Elongation factor 1-α 1 (EF-1-α-1)*	11	99	25	EF1_alpha, EF_GTPbind, EFTU_Cterm, EFTU_D2
sp|P52597	*Heterogeneous nuclear ribonucleoprotein F (hnRNP F)*	2	99	27	RNA_rec_mot
sp|P31943	*Heterogeneous nuclear ribonucleoprotein H (hnRNP H)*	2	99	25	RNA_rec_mot
sp|Q07244	Heterogeneous nuclear ribonucleoprotein K (hnRNP K)	2	99	31	KH_dom, KH_type_1
sp|Q13144	Translation initiation factor eIF-2B ϵ subunit (eIF-2B GDP-GTP)	3	98	22	eIF5C, Hexapep_transf
sp|Q9NR50	*Translation initiation factor eIF-2B γ subunit (eIF-2B GDP-GTP)*	2	99	26	NTP_transferase
	Protein stability, processing, degradation				
sp|P10809	*60 kDa heat shock protein, mitochondrial precursor (Hsp60)*	4	99	27	Chaprnin_Cpn60, GroEL-ATPase
sp|P11021	*78 kDa glucose-regulated protein precursor (GRP 78)*	14	99	33	ER_target_S, Hsp70
sp|P27824	Calnexin precursor (chaperone)	2	99	30	Calret_calnex_P, ConA_like_lac_gl
sp|P22681	*CBL E3 ubiquitin protein ligase*	6	99	29	Cbl_N, UBA_domain, ZF_RING_1
sp|Q13191	*CBL-B (SH3-binding protein CBL-B)*	13	99	26	Cbl_N, SH2, UBA_domain, ZF_RING_1
sp|P31689	*DnaJ homolog A member 1 (Hsp40 protein 4)*	4	99	28	DnaJ_CXXCXGXG, Hsp_DnaJ
sp|O60884	*DnaJ homolog A member 2 (cell cycle progression)*	2	99	22	DnaJ_CXXCXGXG, Hsp_DnaJ
sp|Q96EY1	*DnaJ homolog A member 3 (Tumorous imaginal discs protein)*	2	99	25	DnaJ_CXXCXGXG, Hsp_DnaJ
sp|Q9UBS4	DnaJ homolog B member 11 precursor (ER-associated dnaJ)	2	99	38	DnaJ_CXXCXGXG, Hsp_DnaJ
gi|15812198	F-box only protein 2; F-box protein 2; F-box gene 1	2	98	22	F-box associated region
sp|P04792	*Heat shock 27 kDa protein (HSP 27)*	10	99	39	Hsp20
sp|P08107	*Heat shock 70 kDa protein 1 (HSP70.1)*	5	99	33	Hsp70
sp|P11142	*Heat shock cognate 71 kDa protein*	15	99	33	Hsp70
sp|P08238	*Heat shock protein HSP 90-β (HSP 84) (HSP 90)*	5	99	34	ATPbind_ATPase, Hsp90
sp|P05092	Peptidyl-prolyl cis-trans isomerase A	4	99	26	CSA_PPlase
sp|P38646	*Stress-70 protein, mitochondrial precursor (75 kDa glucose regulated)*	21	99	31	Hsp70
sp|P02248	*Ubiquitin*	3	99	35	Ubiquitin
	Small molecule transport, energy utilization				
sp|P05141	*Adenine nucleotide translocator 2 (solute carrier family 25)*	8	99	27	Mit_carrier, Mit_uncoupling, Mitoch_carrier
sp|P06576	*ATP synthase β chain, mitochondrial precursor*	4	99	37	AAA_ATPase
sp|P56134	ATP synthase f chain, mitochondrial	2	99	31	—
gi|4503571	Enolase 1; phosphopyruvate hydratase; MYC promoter-binding protein	2	99	24	Enolase
sp|P04406	Glyceraldehyde 3-phosphate dehydrogenase	4	99	29	GAP_dhdrogenase, GAPDH-I
sp|Q00325	*Phosphate carrier protein, mitochondrial precursor (PTP)*	4	99	26	Mitoch_carrier
sp|P14786	Pyruvate kinase, M2 isozyme (and/or M1)	2	99	15	Pyruvate_kinase
gi|21361344	*Solute carrier family 3 (4F2 heavy chain; CD98)*	5	99	29	Alpha_amyl_cat
sp|P00938	Triosephosphate isomerase	2	99	17	Triophos_ismrse
sp|P07919	Ubiquinol-cytochrome C reductase complex 11 kDa protein	2	99	23	UCR_hinge
	Transcription, chromatin regulation				
sp|P78527	DNA-dependent protein kinase catalytic subunit	3	99	25	FAT, P13_P14_kinase,
sp|P10412	*Histone H1.4 (Histone H1b)*	4	99	30	Histone_H1/H5
sp|P02278	*Histone H2B*	2	99	35	Hist_TAF, Histone_core_D, Histone_H2A
gi|17402907	*Tripartite motif protein TRIM29 isoform β, ataxia group D-associated*	12	98	33	B-Box-type zinc finger

TABLE I—*continued*

Accession ID	Protein class and name	Unique peptides	Mean % confidence	Mean % score	Select domains
sp|Q03164	Zinc finger protein HRX (ALL-1) (Trithorax-like protein)	2	99	39	Bromodomain, Fynch, SET, Znf_CXXC, Znf_PHD
	Unknown				
sp|P42704	130kDa Leucine-rich protein (Irp 130) (gp 130)	2	99	22	Prenyl_trans, TPR-like
gi|7106299	*Like mouse brain protein E46 (possible b-catenin-like)*	3	99	26	Uncharacterized conserved protein
sp|P40855	*Peroxisomal farnesylated protein (33 kDa housekeeping protein)*	3	99	29	Pex19
gi|19920317	*Transmembrane protein (63kD), endoplasmic reticulum/Golgi interm*	3	97	27	Myosin class II heavy chain
	Vesicle transport				
sp|O75843	Adapter-related protein complex 1 γ 2 subunit	2	99	28	A/G_adapt_C, Adaptin_N, Gamma_adaptin_C
sp|Q13438	Protein OS-9 precursor (amplified in osteosarcoma)	2	99	34	Man_6_P_R_bind

RESULTS

Immunoaffinity Enrichment of Tyrosine-phosphorylated and EGF Receptor-associated Proteins and Complexes—Phosphotyrosine-containing proteins and complexes were isolated and identified, using the HN5 HNSCC line as a model system. Constitutive EGF receptor signaling has been associated with altered signaling resulting in cell transformation and HN5 cells, expressing $\sim 5 \times 10^6$ receptors per cell (20), show high-constitutive EGF receptor kinase activity due to autocrine TGF-α expression. From multiple biological experiments 774 unique peptides were identified and manually confirmed, corresponding to 236 proteins, not including trypsin, immunoglobulin, fetuin, or bovine serum albumin ($\sim$27 peptides in total). The mean ProID/ProICAT peptide confidence and score were 99 and 29%, respectively. The 125 proteins identified with two or more peptides are listed in Table I and the peptide coverage of EGF receptor is listed in Table II. Protein assignments, confidence levels and scores for all peptides are shown in Supplemental Table I. Average errors in peptide mass measurements within information-dependent MS and MS/MS experiments using an qQ-TOF instrument were generally $<$0.05 Da and resolution values $>$9,000 allowed accurate charge state calculation. Nevertheless all assigned fragment ion peptide spectra were verified by visual inspection. Proteins were grouped using simplified Gene Ontology (GO; www.geneontology.org) process terms (Table I) where focal adhesion, microtubule, keratin filament, and actin filament proteins were bundled.

In HN5 cells the EGF receptor was the predominant phosphoprotein detected by anti-pY immunoblot (Fig. 2*A*), which was overexposed to reveal phosphorylated substrates whose phsophorylation could be prevented by inhibition of EGF receptor kinase activity. The EGF receptor showed the best peptide coverage by LC-MS/MS (defined by 80 peptides and 7 phosphopeptides; Table II) and by MALDI analysis (defined by 36 peptides; Table II). In this model system, EGF receptor represented the major scaffolding protein by which associated proteins and phosphoproteins were enriched. The three most-abundant classes of proteins observed (Table I and Fig. 3) were those associated with cell adhesion and cytoskeletal organization (43 proteins), mitogenesis and cell survival (23 proteins), and protein stability and degradation (17 proteins). In addition, two smaller-scale anti-EGFR affinity chromatography experiments also were performed where the monoclonal antibody (EGFR.1), recognizing an extracellular domain EGF receptor epitope, was used for protein selection. These experiments yielded 69 proteins in common with those identified by anti-pY affinity selection, and these are shaded gray in Table I.

EGF Receptor Phosphorylation—Both known and unreported phosphopeptides from both unstimulated and EGF hyperstimulated cells could be readily identified from complex protein mixtures in both LC-MS/MS and MALDI workflows (Table III). These phosphopeptides were not detected when EGF receptor kinase activity was inhibited with erlotinib. Tyrosine phosphorylation of the four major autophosphorylation sites at positions Y1173 (P1), Y1148 (P2) (21), Y1114 and Y1086 (P4; Ref. 22) was observed within these complex peptide mixtures, with high ion counts and fragment ion coverage (Fig. 4). Phosphorylation of Y974 was observed (Table III) in both LC-MS/MS (2^+ and 3^+ ions) and MALDI studies (1^+ ions), yielding a predicted SH2 interaction motif (ScanSite; scansite.mit.edu). Fragment ion spectra also indicated that S967 also could be phosphorylated within the same peptide, though co-phosphorylation of both sites was not observed. *In vitro* phosphorylation of anti-EGFR immune complexes with active Src kinase identified two additional EGFR phosphopeptides Y740 EILDEA(pY)VMASVDNPHVCR and Y703 VLGSGAFGTV(pY)K, though these could not detected directly from cell extracts. Immunoblot studies showed inhibition of EGF receptor autophosphorylation by erlotinib markedly decreased phosphophorylation of EGF receptor at sites Y845, Y992, Y1045, and Y1068 within the C-terminal SH2/PTB interaction domain (Fig. 5). ICAT labeling showed tyrosine phosphorylation at Y1086 and Y1148 in both the EGF treatment and no treatment control HN5 cells, but not after inhi-

TABLE II

EGF receptor peptides identified by LC-MS/MS and MALDI methods using multiple search engines, ProID/ProICAT, SONAR, and Mascot for fragment ion spectra and Knexus for MALDI data (<30 ppm)

Epidermal growth factor receptor peptides	ProID confidence (%)	ProID score	SONAR exp value	Mascot score	Sequence position	MALDI <30 ppm
ACGADSYEMEEDGVR	99	56	1.5 × 10−4	80	286–300	+
ACGADSYEMEEDGVRK	99	50	1.1 × 10−6	38	286–301	
ANKEILDEAYVMASVDNPHVCR	98	21	–	–	731–752	
ATGQVCHALCSPEGCWGPEPR	99	38	2.7 × 10−5	36	477–497	+
CEGPCR	99	11	–	–	305–310	
CEGPCRK	95	14	–	–	305–311	
CNLLEGEPR	99	22	1.1 × 10−2	45	515–523	+
CWMIDADSRPK (and/or erbB4)	99	37	3.0 × 10−4	50	926–936	+
DCVSCR	99	14	7.6 × 10−1	–	498–503	+
DEATCK	99	15	–	–	232–237	
DEATCKDTCPPLMLYNPTTYQMDVNPEGK	–	–	4.9 × 10−3	–	232–260	
DNIGSQYLLNWCVQIAK (pY789)	99	42	8.6 × 10−4	40	783–799	+
DPHYQDPHSTAVGNPE(pY)LNTVQPTCVNSTFDSPAHWAQK (pY1114)	99	9	–	11	1098–1136	
DPHYQDPHSTAVGNPEYLNTVQPTCVNSTFDSPAHWAQK	99	9	4.9 × 10−3	11	1098–1136	
EAKPNGIFKGSTAENAE(pY)LR (P1: 1173)	99	25	3.8 × 10−1	–	1156–1175	
EAKPNGIFKGSTAENAEYLR	99	34	6.1 × 10−4	–	1156–1175	
ECVDKCNLLEGEPR	99	31	7.0 × 10−1	37	510–523	
EDSFLQR	99	32	4.0 × 10−1	43	1038–1044	+
EHKDNIGSQYLLNWCVQIAK	99	30	2.2 × 10−3	44	780–799	
EILDEAYVMASVDNPHVCR	99	60	4.6 × 10−8	76	734–752	+
EISDGDVIISGNK	99	36	2.8 × 10−2	59	431–443	+
ELIIEFSK	99	41	1.4 × 10−1	46	939–946	+
ELVEPLTPSGEAPNQALLR	99	42	3.4 × 10−22	65	663–681	+
ESDCLVCR	99	14	1.7 × 10−0	20	221–228	+
ESDCLVCRK	98	16	–	–	221–229	
EYHAEGGKVPIK	99	33	1.1 × 10−2	–	844–855	
FRDEATCK	99	40	1.9 × 10−2	16	230–237	
FRELIIEFSK	99	34	–	44	937–946	+
FSNNPALCNVESIQWR	99	55	4.3 × 10−6	75	126–141	+
GDSFTHTPPLDPQELDILK	99	46	3.7 × 10−30	46	354–372	+
GENSCK	99	13	3.7 × 10−1	11	471–476	
GLWIPEGEK	99	48	1.2 × 10−1	28	705–713	+
GLWIPEGEKVK	99	28	2.3 × 10−2	–	705–715	
GMNYLEDR	99	40	6.2 × 10−3	48	800–807	+
GNMYYENSYALAVLSNYDANK	99	36	2.2 × 10−4	57	85–105	
GNMYYENSYALAVLSNYDANKTGLK	99	30	–	–	85–109	
GPDNCIQCAHYIDGPHCVK	99	31	9.2 × 10−3	21	551–569	
GRECVDK	98	32	1.2 × 10−1	–	508–514	
GSHQISLDNPD(pY)QQDFFPK (P2: 1148)	99	40	–	36	1137–1155	+
GSHQISLDNPDYQQDFFPK	99	46	1.4 × 10−3	42	1137–1155	
GSTAENAE(pY)LR (P1: 1173)	99	28	–	–	1165–1175	+
GSTAENAEYLR	99	32	5.0 × 10−2	41	1165–1175	
IICAQQCSGR	99	24	7.0 × 10−2	–	189–198	+
IISNRGENSCK	99	24	–	–	466–476	
IKVLGSGAFGTVYK	99	40	6.8 × 10−5	31	691–704	
ILKETEFK	99	27			682–689	
IPLENLQIIR	99	55	2.1 × 10−31	60	75–84	+
IPSIATGMVGALLLLLVVALGIGLFMR	98	17	1.0 × 10+3	–	619–645	
ITDFGLAK	99	44	6.0 × 10−2	54	829–836	+
IYTHQSDVWSYGVTVWELMTFGSKPYDGIPASEISSILEK	99	17	–	26	866–905	
KCEGPCR	99	20	–	–	304–310	
KVCNGIGIGEFK	99	56	1.1 × 10−4	53	311–322	+
KVCQGTSNK	99	21	3.8 × 10−2	20	005–013	
LLQERELVEPLTPSGEAPNQALLR	99	32	–	–	658–681	
LPQPPICTIDVYMIMVK (pY920; and/or erbB2)	99	37	6.7 × 10−4	41	909–925	
LTQLGTFEDHFLSLQR	99	48	4.8 × 10−62	61	014–029	+
MHLP(pS)PTDSNFYR (pS967)	99	27	–	–	963–975	+

TABLE II—*continued*

Epidermal growth factor receptor peptides	ProID confidence (%)	ProID score	SONAR exp value	Mascot score	Sequence position	MALDI <30 ppm
MHLPSPTDSNF(pY)R (pS974)	99	29	–	–	963–975	+
MHLPSPTDSNFYR	99	44	$1.7 \times 10-2$	51	963–975	+
NGLQSCPIK	99	20	–	–	1029–1037	
NGLQSCPIKEDSFLQR	99	55	$2.3 \times 10-5$	40	1029–1044	+
NLCYANTINWK	99	42	$1.5 \times 10-3$	36	444–454	
NLCYANTINWKK	99	40	$8.0 \times 10-2$	–	444–455	
NLQEILHGAVR	99	51	$1.6 \times 10-41$	65	115–125	+
NVLVKTPQHVK	99	37	$5.0 \times 10-3$		818–828	
NYDLSFLK	99	32	$2.8 \times 10-1$	42	049–056	+
NYDLSFLKTIQEVAGYVLIALNTVER	99	29	–	–	049–074	
NYVVTDHGSCVR	99	56	$7.2 \times 10-5$	30	274–285	+
RPAGSVQNPV(pY)HNQPLNPAPSR (P4: 1086)	99	75	–	46	1076–1097	+
RPAGSVQNPVYHNQPLNPAPSR	99	60	$6.6 \times 10-6$	50	1076–1097	+
SLKEISDGDVIISGNK	99	52	$4.9 \times 10-4$	58	428–443	+
SPSDCCHNQCAAGCTGPR	99	28	–	–	203–220	
TDLHAFENLEIIR	99	55	$3.9 \times 10-32$	60	428–443	+
TIQEVAGYVLIALNTVER	99	60	$1.0 \times 10-4$	86	057–074	+
TPLLSSLSATSNNSTVACIDR	99	60	$2.4 \times 10-5$	91	1008–1028	
VAPQSSEFIGA	97	21	–	17	1176–1186	
VCNGIGIGEFK	99	47	$6.3 \times 10-4$	56	312–322	+
VCQGTSNK	90	30	$8.0 \times 10-2$	28	006–013	
VKIPVAIK	99	38	$6.0 \times 10-2$	34	714–721	
VLGSGAFGTVYK (also erbB2)	99	55	$4.2 \times 10-42$	75	693–704	+
VLGSGAFGTVYKGLWIPEGEK (pY703)	99	27	–	–	693–713	
VPIKWMALESILHR	99	37	–	53	852–865	
WMALESILHR	99	44	$9.5 \times 10-6$	48	856–865	+
YLVIQGDER (pY964)	99	46	$3.0 \times 10-22$	51	954–962	+
YSFGATCVK	99	26	$2.0 \times 10-33$	35	261–269	+
YSFGATCVKK	99	25	$1.5 \times 10-4$	15	261–270	
YSSDPTGALTEDSIDDTFLPVPEYINQSVPK	99	27	$5.0 \times 10-3$	–	1045–1097	

bition of EGF receptor kinase activity. The inhibition of EGF receptor kinase activity increased total EGF receptor levels (Fig. 5, *left*), most likely by attenuating autophosphorylation-dependent internalization.

EGF receptor can be tyrosine-phosphorylated at combinations of at least 12 sites in cells, and this high stoichiometry contributes to complexity in interactions, both with phosphotyrosine binding signaling partners and with the anti-pY affinity resin used for protein isolation. For example when erlotinib treatment (1 μM, 60 min) was followed by EGF stimulation (10 ng/ml, 10 min) prior to cell lysis and anti-pY affinity selection, marked down-regulation of EGF receptor in the anti-pY fraction was observed both by ICAT labeling (76 $\pm$ 4%; Table IV) and by immunoblot (Fig. 2*A*). However in the absence of exogenous EGF, little difference between control and erlotinib was observed by ICAT labeling (102 $\pm$ 4%; Table IV) in two biological experiments and multiple LC-MS/MS experiments. In the absence of EGF stimulation, the EGF receptor appeared to dephosphorylate relatively slowly and incompletely following erlotinib treatment, where sufficient tyrosine phosphate was present on EGF receptor to bind the pY affinity resin with similar efficiency as the control sample. This contrasted with rapid reduction in EGF receptor-interacting phosphoproteins such as Cbl-B, Erk1/2, PLCγ, and Vav-2 with erlotinib treatment in the absence of exogenous EGF (Table IV). This also contrasted with our finding with the constitutively active juxtamembrane mutant Kit receptor tyrosine kinase, where >80% dephosphorylation of the receptor rapidly occurs within 60 min of pharmacological Kit kinase inhibition, directly paralleling anti-pY capture of Kit (data not shown). These data suggest that whole-protein phosphotyrosine capture methods are also sensitive to the stoichiometry of protein phosphorylation and to the rates of dephosphorylation of the individual phosphorylation sites.

Activation and Inhibition of EGF Receptor Kinase Activity Modulates Proximal Signaling Components—The relative abundance of phosphotyrosine-containing proteins and complexes from the HNSCC cell line HN5 were measured by immunoblot and by ICAT labeling from multiple biological experiments. Two types of experiments were performed. First, experiments were performed where EGF receptor kinase activity was inhibited by the selective EGFR kinase inhibitor erlotinib (1 μM for 60 or 120 min) with or without exogenous ligand (EGF 10 ng/ml for 10 min) prior to lysis and anti-pY affinity selection. In a second paradigm, EGF receptor was hyperstimulated with exogenous EGF ligand (10 ng/ml for

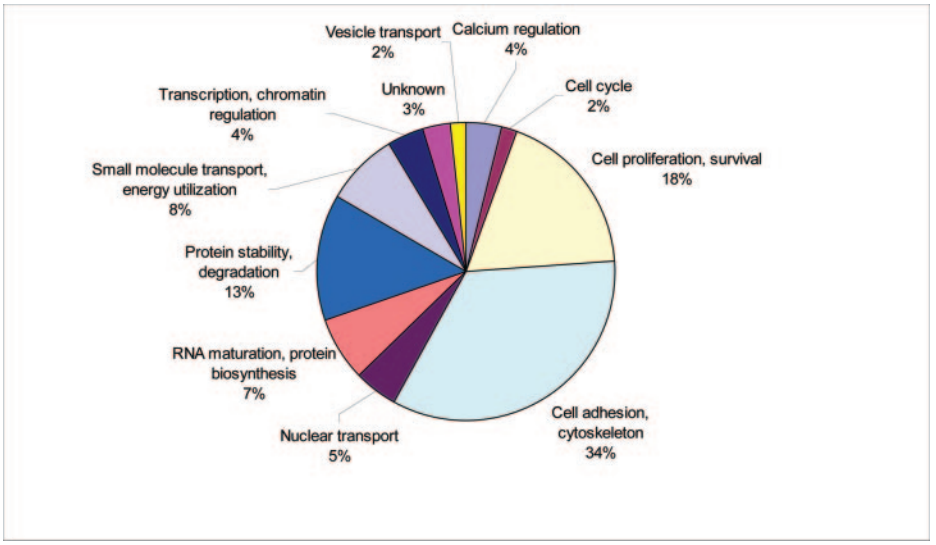

FIG. 3. **Protein functional classes identified from anti-pY affinity selection and LC-MSMS fragment ion spectra database searching.**

TABLE III

Phosphopeptides identified by LC-MS/MS with percent confidence, score, best ScanSite motif prediction and identified nonphosphorylated peptide counterparts

Phosphoprotein (residue)	Peptide	Confidence (%)	Score	ScanSite (percentile)
Paxillin				
pY118	VGEEEHV(pY)SFPNK	99	42	Crk-SH2 (0.24%)
	VGEEEHVYSFPNK	99	44	
pY88	FIHQQPQSSSPV(pY)GSSAK	99	36	Src (3.3%)
	FIHQQPQSSSPVYGSSAK	99	40	
p130CAS				
pY249	HLLAPGPQDI(pY)DVPPVR	99	21	Crk-SH2 (0.01%)
pY306	GLPPSNHHAV(pY)DVPPSVSK	99	28	Nck_SH2 (0.05%)
pY387	RPGPGTL(pY)DVPR	99	30	Abl (0.01%)
RPGPGTLYDVPR	99	32		
EGF receptor				
pY1173 P1	EAKPNGIFKGSTAENAE(pY)LR	99	25	EGFr (0.05%)
	EAKPNGIFKGSTAENAEYLR	99	34	
pY1173 P1	GSTAENAE(pY)LR	99	28	EGFr (0.05%)
	GSTAENAEYLR	99	32	
pY1148 P2	GSHQISLDNPD(pY)QQDFFPK	99	40	EGFr (0.23%)
	GSHQISLDNPDYQQDFFPK	99	46	
pY1086 P4	RPAGSVQNPV(pY)HNQPLNPAPSR (P4: 1086)	99	75	EGFr (1.05%)
	RPAGSVQNPVYHNQPLNPAPSR (P4: 1086)	99	60	
pY1114	DPHYQDPHSTAVGNPE(pY)LNTVQPTCVNSTFDSPAHWAQK	99	9	EGFr (0.04%)
	DPHYQDPHSTAVGNPEYLNTVQPTCVNSTFDSPAHWAQK	99	9	
pY974	MHLPSPTDSNF(pY)R	99	25	
	MHLPSPTDSNFYR	99	44	
pS967	MHLP(pS)PTDSNFYR	99	27	p38MAPK (1.40%)
	MHLPSPTDSNFYR	99	44	

1, 3, or 15 min) prior to phosphoprotein isolation. In both cases, the cleavable ICAT cysteine labeling method was used to allow relative quantitation of proteins isolated under the different biological conditions. Treatment and control protein samples were separately labeled with heavy isotopic or light isotopic mass labels, respectively, degraded with trypsin and subjected to LC-MS/MS. ICAT labeling and subsequent recovery of only cysteine-derivitized peptides further reduced sample complexity. From erlotinib-treated or EGF-hyper-stimulated cells, 33 proteins were measured by ICAT labeling and 26 proteins were measured by immunoblot. These data are summarized in Table IV. The majority of proteins were unaltered by more than 30% in representation after erlotinib (69% of proteins) or EGF (53% of proteins) exposure *in vitro*.

EGF receptor autophosphorylation establishes binding sites for proteins containing SH2 and PTB domains (7). Multiple SH2 domain-containing proteins were modulated by erlotinib and/or EGF exposure (Table IV), and these were

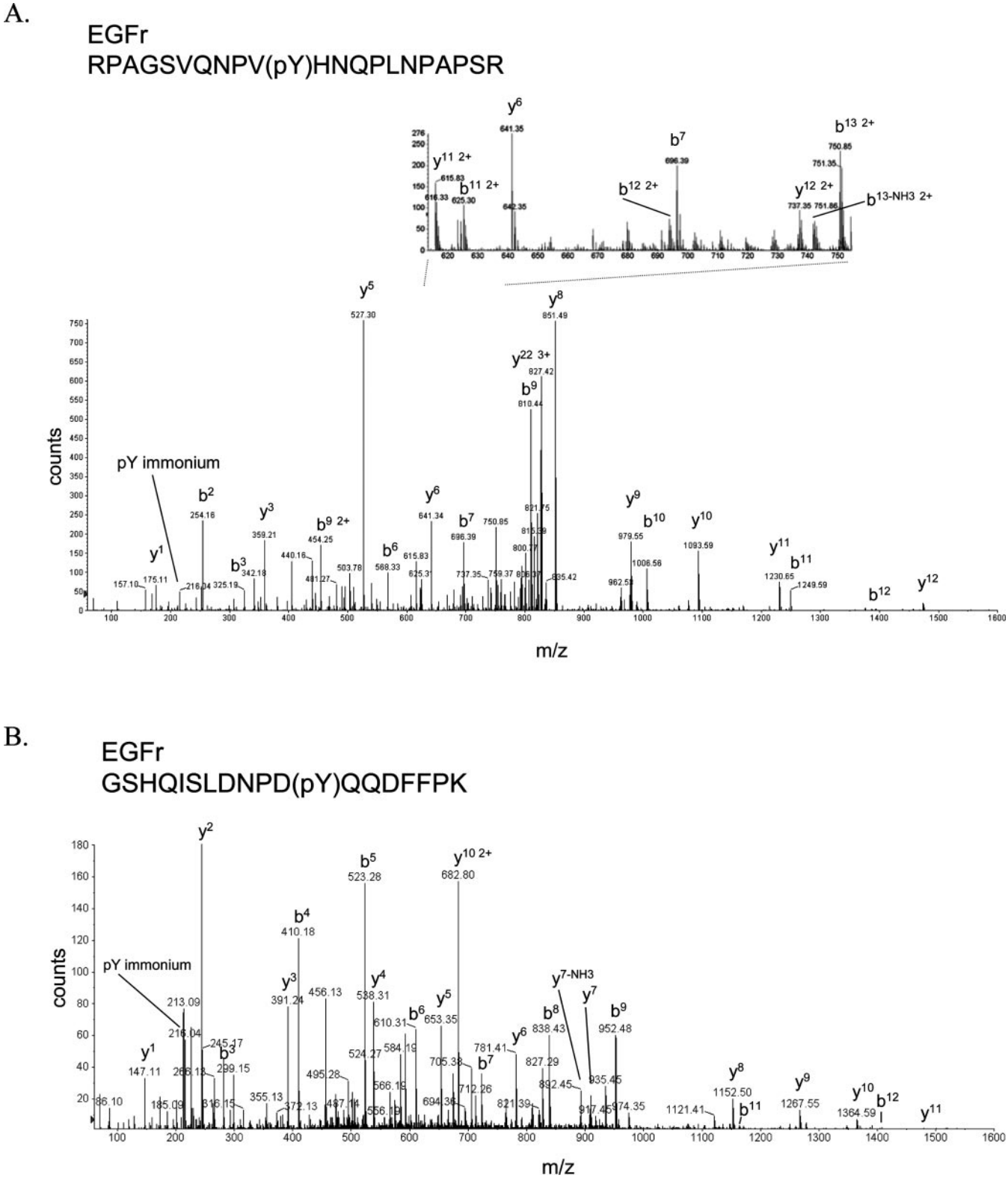

FIG. 4. *A*, anti-pY affinity selection and fragment ion spectra of the EGF receptor peptide RPAGSVQNPV(pY)HNQPLNPAPSR autophosphorylated on Y1086 from a complex peptide mixture. *B*, anti-pY affinity selection and fragment ion spectra of the EGF receptor peptide GSHQISLDNPD(pY)QQDFFPK autophosphorylated on Y1148 from a complex peptide mixture.

FIG. 5. **EGF receptor inhibition by erlotinib (OSI-774; 1 μM, 2 h) reduced EGFR autophosphorylation at Y992, Y1048, and Y1068, the phosphorylation of erbB2 and phosphorylation of EGFR Y845 by Src family kinases by immunoblot of the anti-pY affinity fraction.**

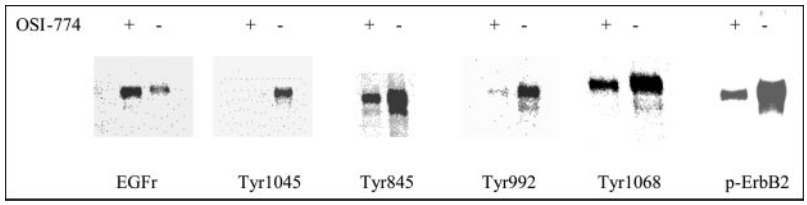

TABLE IV

Protein quantitation of the anti-pY fraction from HN5 cells by ICAT labeling and immunoblot approaches, in which the EGF receptor kinase was either inhibited with erlotinib or stimulated with EGF

Data are presented as fold stimulation. Standard errors are in parentheses. NC denotes no observable change by immunoblot.

Accession ID	Protein name	Erlotinib (Immunoblot) 120 min	Erlotinib (ICAT) 120 min	Erlotinib + EGF (ICAT) 60 min	EGF 1 min	EGF 3 min	EGF 15 min
sp|P29312	14-3-3 protein ζ (protein kinase C inhibitor protein-1)	NC	1.1 (0.0)		1.3 (0.1)	1.3 (0.1)	
sp|P05141	Adenine nucleotide translocator 2 (solute carrier family 25)					1.1 (0.1)	
sp|Q14161	ARF GTPase-activating protein GIT1				0.9 (0.1)	0.6 (0.0)	0.6 (0.0)
sp|O60716	Catenin Δ-1 (p120 catenin) (p120(ctn)) (cadherin-associated Src)		1.3 (0.1)			2.3	2.0 (0.2)
sp|Q13191	CBL-B (SH3-binding protein CBL-B)		0.3		1.6 (0.1)		2.4 (0.1)
gi|4758046	Cell cycle progression 2 protein					1.1	1.1 (0.0)
sp|P56945	CRK-associated substrate (p130Cas)	↓	0.9		0.8 (0.1)	0.5 (0.0)	0.7 (0.0)
gi|30410805	CUB domain-containing protein 1 isoform 1 (SIMA135/CDCP1)		1.1 (0.1)		1.1 (0.0)	0.9 (0.1)	0.9 (0.1)
sp|P04720	Elongation factor 1-α 1 (EF-1-α-1)		1.2			1.2	1.5 (0.1)
sp|P29317	Ephrin type-A receptor 2 precursor	↓	0.8				
sp|P98172	Ephrin-B1 precursor (EPH-related receptor tyrosine kinase ligand 2)		1.0				
sp|Q05397	Focal adhesion kinase 1 (FADK 1) (pp125FAK; PTK2)	↓	0.4		0.5 (0.0)		
sp|P09382	Galectin-1 (β-galactoside-binding lectin L-14-I)		1.2 (0.3)		1.0 (0.1)	1.5 (0.1)	1.4 (0.1)
sp|O00410	Importin β-3 subunit (Karyopherin β-3 subunit) (Ran-binding)	↑			1.0 (0.1)		
sp|Q14192	LIM-protein 3 (SLIM 3) (LIM-domain protein DRAL)		1.0 (0.1)				
sp|Q16539	Mitogen-activated protein kinase 14		1.0 (0.0)				
sp|P27361	Mitogen-activated protein kinase 3; (and/or MAPK1; Erk 1,2)	↓	0.4	0.0			2.0 (0.1)
gi|4885525	NSP1; SH2 domain containing 3A; novel SH2-containing protein 1		1.1		1.2 (0.1)	0.80 (0.1)	1.0 (0.0)
gi|4502371	NSP2; breast cancer antiestrogen resistance 3		0.8 (0.1)				0.9 (0.0)
sp|P49023	Paxillin	↓	1.0	0.4			
sp|Q00325	Phosphate carrier protein, mitochondrial precursor (PTP)				1.3 (0.1)	1.2 (0.1)	
sp|P19174	PLCγ1; 1-phosphatidylinositol-4,5-bisphosphate phosphodiesterase γ		0.0				1.2
sp|Q99959	Plakophilin 2	↓					2.7 (0.1)
sp|P07947	Proto-oncogene tyrosine-protein kinase YES (p61-YES)	NC	1.0				
sp|P31949	S100 calcium-binding protein A11 (Calgizzarin)		1.0				
sp|P29353	SHC transforming protein	↓		0.0	1.1 (0.1)		1.0 (0.0)
sp|P38646	Stress-70 protein (75-kDa glucose regulated)		2.0				
sp|Q13144	Translation initiation factor eIF-2B epsilon subunit (eIF-2B GDP-GTP)		1.2 (0.0)		1.0 (0.0)	0.9 (0.1)	1.1 (0.1)
gi|17402907	Tripartite motif protein TRIM29 isoform β; ataxia-telangiectasia group D		0.8				
sp|P07919	Ubiquinol-cytochrome *c* reductase complex 11 kDa, mitochondrial		0.9 (0.1)		1.1	0.8	
sp|P52735	Vav-2 protein		0.0				
sp|P00533	Epidermal growth factor receptor precursor Phospho-EGFR	↑ ↓	1.0 (0.0)	0.2 (0.0)			
sp|P04626	Receptor protein-tyrosine kinase erbB-2 precursor Phospho-ErbB2	 ↓	1.1 (0.0)	0.2 (0.0)			

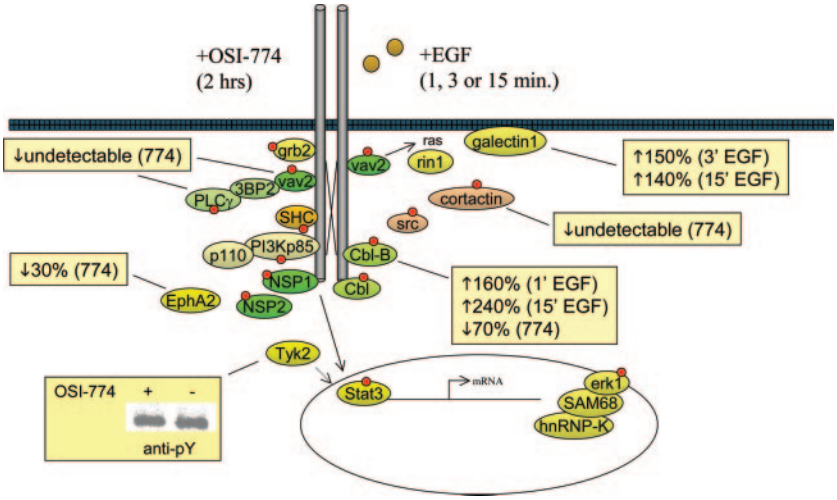

FIG. 6. **Proteins associated with proximal EGF receptor signaling and their modulation by transient exposure to EGF (10 ng/ml 10 min) or to erlotinib (OSI-774; 1 μM for 120 min) and were modeled using present data, Network Explorer (Ingenuity), and literature data.**

modeled using the pathway connectivity Network Explorer software, from data obtained by anti-EGFR selection and from data obtained from the literature (Fig. 6). Competition between the anti-pY antibody and SH2/PTB phosphotyrosine binding proteins, which might restrict the detection SH2/PTB domain proteins, was not apparent. Vav2 and PLCγ were both acutely down-regulated by erlotinib, where only the D_0 control peak could be detected and sequenced. The converse was true for Vav2, where upon exposure to EGF only the D_9 treatment group labels were observed. The isolation of caveolin-1 in both anti-pY and anti-EGF receptor affinity fractions supports EGF receptor co-localization within caveolae. The activation of EGF receptor substrates PLCγ and PI-3 kinase substrates is thought to occur within lipid raft membrane compartments including caveolae (23). Consistent with this interpretation, caveolin-1 recovery within the anti-pY fraction was reduced by EGF receptor blockade (Fig. 7*B*). It has been proposed that PLCγ activation results in calcium mobilization within caveolae and subsequent activation of calcium dependent enzymes such as the S100 family members selected by anti pY affinity.

The MAP kinases Erk-1 and -2 are connected to EGF receptor signaling through the Ras-Raf-Mek pathway. As expected, kinase blockade reduced Erk representation by at least 68%, where the treatment D_9 peak was undetectable in two experiments (Table IV). The erlotinib reduction in Erk phosphorylation was qualitatively consistent with those obtained by immunoblot (Fig. 8). Hyperstimulation of EGF receptor activity by exogenous EGF increased Erk 200% somewhat late (15 min) after stimulation. The E3 ubiquitin ligase Cbl, which interacts with EGF receptor through the adapter Grb2, functions as a key negative regulator by promoting ubiquinylation and proteosomal destruction of the receptor. Both Cbl-E3 ligase and Cbl-B proteins were found in the anti-pY fraction, and Cbl-B was additionally observed in the anti-EGF receptor fraction (Table I). The abundance of Cbl-B in the phosphotyrosine fraction was reduced 73% by EGF receptor kinase inhibition and was increased by EGF treatment 160 and 240% after 1 and 15 min exposure, respectively. Additional components of internalization and proteosomal degradation complexes were identified, including the 26S proteosomal regulatory subunit-2 (by both LC-MS/MS and immunoblot), the F-box only protein-2, S100A6, calcyclin binding protein and ubiquitin (by LC-MS/MS), and dynamin, cullins 1 and 2, clathrin heavy chain, and the ubiquitin C-terminal hydrolase (by immunoblot; data not shown).

Alternative approaches to the dissection of EGF receptor signaling have been reported (24–27). Stable isotope-labeled proteins from the EGF-stimulated cervical carcinoma cell line HeLa ($\sim 2 \times 10^5$ receptors/cell) were selected by Grb2-SH2 domain affinity, fractionated by SDS-PAGE, and peptides subjected to LC-MS/MS. The Grb2-SH2 domain shows preference for pYKNI/L, is permissive for pYXNX, and interacts with EGF receptor at multiple positions. Due to the involvement of Grb2 in EGF receptor signaling, we examined the cross-identification of proteins between the two studies. Of the 228 proteins identified by Grb2-SH2 interaction in HeLa cells (24), ~49 (21%) were common in the full phosphotyrosine affinity fractions characterized here (Supplemental Table I). Of those proteins modulated by ligand stimulation of EGF receptor, Shc, Grb2, Vav-2, Cbl-B, polyubiquitin, actin, keratin-17, and plectin-1 were common between the two studies. A previous study using phosphotyrosine precursor ion scanning of HeLa cell anti-pY selected proteins, separated by SDS-PAGE, identified 10 proteins, four of which were common to the study here (EGF receptor, Cbl, Hsp70, and Shc; Ref. 25). Similarly, anti-pY and two-dimensional gel electrophoretic approaches to mapping of A431 cell proteins yielded 16 proteins overlapping with those reported here (comprising EGFR, PLCγ, α_6-integrin, γ-catenin, PI-3 kinase p85β, ezrin, Grp78, cortactin, Hsp71, Grp75, α-tubulin, Shc, actin, and Grb2) out of 19 proteins in total (26). These differences suggest diversity between the HeLa, A431, and HN5 cell systems and the different methodologies employed.

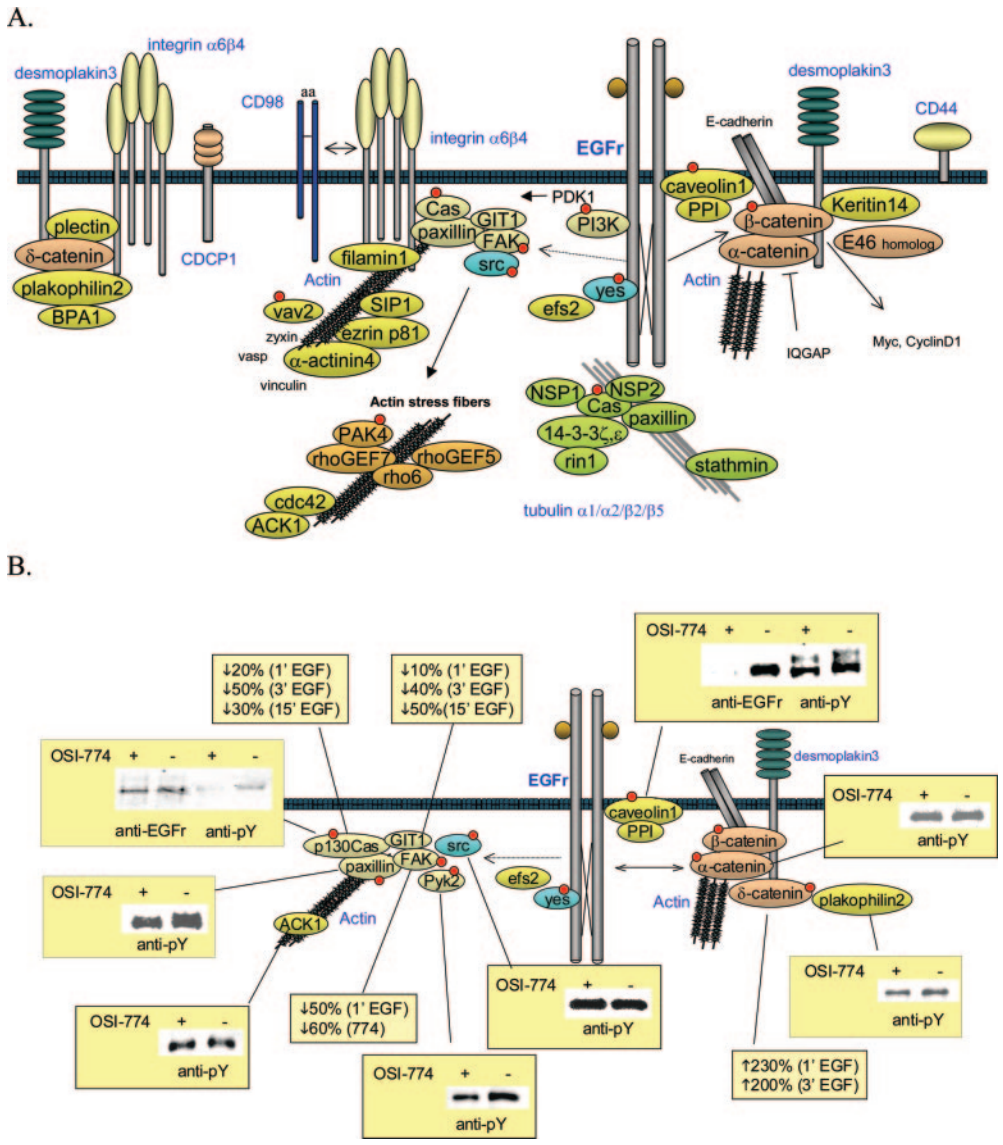

FIG. 7. **Proteins and complexes implicated in cell adhesion and cell-cell contact (*A*) and their modulation (*B*) by transient exposure to EGF (10 ng/ml 10 min) or to erlotinib (OSI- 774; 1 μM for 120 min) and were modeled using present data, Network Explorer (Ingenuity), and literature data.**

Tyrosine Phosphorylation Contributed by Non-EGF Receptor Protein Kinases—Twelve tyrosine protein kinases and three serine-threonine protein kinases, from multiple functional categories, were among the proteins isolated by anti-pY) affinity chromatography. Despite the dominant role of EGF receptor in the model cell system used, FAK (19 peptides), ErbB2 (7 peptides), c-Yes (7 peptides), c-Src (6 peptides), IGF-1 receptor (2 peptides), Pyk2 (3 peptides), EphA2 (7 peptides), EphB3 (3 peptides), EphB4 (2 peptides), and ACK1 (4 peptides) likely also influence the proteins selected by anti-pY affinity chromatography. ErbB2, Yes, FAK, EphA2, EphB4, and ACK1 also were also observed by anti-EGFR affinity selection.

As a consequence, we considered the relative contributions of these tyrosine kinases to the proteins and complexes isolated and considered the extent of cross-talk between kinases. For example activation of EGF receptor, by ligand or by mutation, has been shown to result in the activation of Src, through indirect phosphorylation of the activating Src Y419 site within the kinase activation loop. In turn, activated Src is known to phosphorylate EGF receptor on Y845 and Y1101 (28), thereby recruiting signaling proteins. The activation of Src and Yes kinases was indicated by several pieces of evidence. First, EGF receptor was phosphorylated on Y845, a known Src phosphorylation site (Fig. 5). Second, Src phosphorylation at Y419, required for full kinase activity, was observed by immunoblot (Fig. 7*B*) and was strongly suggested by LC-MS/MS (data not shown). Third, p130CAS was phos-

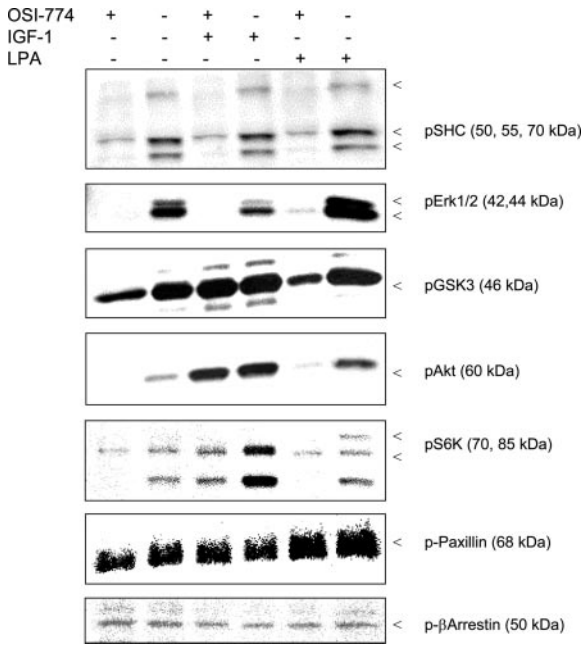

FIG. 8. **EGF receptor, IGF-1 receptor, and LPA signaling cross-talk in HN5 cells, where LPA signaling requires Src for coupling to EGF receptor.** The selective EGF receptor inhibitor erlotinib (OSI-774; 1 μM for 120 min), IGF-1 (10 ng/ml for 30 min), and LPA (1 μM for 30 min) were added to media containing 10% fetal calf serum. EGF receptor blockade by erlotinib reduced pERK, pShc, pGSK-3, and pAkt. The erlotinib-mediated reduction in pGSK-3 and pAkt was attenuated by addition of exogenous IGF-1, but not by addition of LPA, which requires Src family and EGF receptor activities for signaling through PI3-kinase and MAP kinase pathways. Phospho-paxillin was increased by LPA addition and modestly inhibited by EGF receptor inhibition (OSI-774). No change in β-arrestin was observed.

phorylated on multiple Src family sites with the central tyrosine-rich domain (Table III). LPA is a mitogen known to use Src and EGF receptor to transduce signals initiated by LPA binding to its G-protein coupled receptors (28–31). LPA addition to HN5 cells increased phospho-Erk and phospho-Akt (Fig. 8), which could be blocked by the selective EGF receptor kinase inhibitor erlotinib. Erlotinib treatment reduced phosphorylation of the EGF receptor at Y845, a site phosphorylated by Src kinases, consistent with a cross-activation of EGF receptor and Src family members (32, 33). However, no change in phospho-Src family Y419 (active state; Fig. 7*B*), phospho-Src Y530 (repressed state), or anti-pY Yes could be detected by immunoblot even after 120 min of EGF receptor kinase inhibition (data not shown). These data suggest a more rapid dephosphorylation of EGF receptor Y845 relative to Src Y419, or distinct compartmentalization of the EGF receptor and Src family kinases (8).

IGF-1 receptor was identified by anti-pY selection from HN5 cells and exogenous IGF-1 increased phospho-Akt and phospho-GSK3, but antagonized phosphorylation of Erk (Fig. 8). However, the phosphorylation of Shc was still effectively blocked by erlotinib (OSI-774), indicating its phosphorylation was largely EGF receptor-dependent and was not perturbed by LPA or IGF-1. Interestingly, the IGF-1-dependent phosphorylations of GSK-3β and Akt could not be overcome through EGF receptor inhibition, indicating IGF-1 activation of the PI-3 kinase pathway was insensitive to EGF receptor blockade. LPA stimulated phospho-paxillin levels while erlotinib modestly decreased paxillin phosphorylation (Figs. 7*B* and 8). No alteration in β-arrestin was observed under these conditions (Fig. 8).

Modulation of Cell Adhesion Complexes by Activation and Inhibition of EGF Receptor Kinase Activity—Cell adhesion proteins including Crk-associated substrate (p130CAS), focal adhesion kinases (FAK and Pyk), and paxillin were readily observed in anti-pY LC-MS/MS and immunoblot experiments. These proteins were shown to form stable interactions with EGF receptor by anti-EGFR affinity selection. Both paxillin and p130CAS have been shown to directly interact with FAK (34), as part of a complex with actin required for focal adhesion assembly. Two phosphopeptides from paxillin were observed (Table III), comprising one known site at Y118 and one unreported site at Y88, N-terminal to the FAK-binding domains and LIM domains. The major paxillin phosphorylation site at Y31 is resident within a peptide mass of 6,031 Da, somewhat too large to be readily detected in the LC-MS/MS scheme used. p130CAS contains an N-terminal FAK-interacting SH3 domain, a centrally located substrate-interacting (Crk) repeat region with multiple tyrosine residues, followed by a C-terminal Ser region responsible for Src binding. Within the central region, tyrosine phosphorylation was unequivocally observed at sites Y249, Y306, and Y387 in the motif YDVP (Table III) and was strongly suggested for Y410 within the motif YAVP (data not shown). The tyrosine phosphorylation of the YDVP motif has been shown to be phosphorylated *in vitro* by Src (35), while direct phosphorylation of this motif by EGF receptor has not been reported.

The assembly of focal adhesion complexes containing FAK/Pyk2, paxillin, p130CAS, and ARF-GIT1 is thought to be regulated through phosphorylation and dephosphosphorylation in a closely balanced manner (13). The anti-pY capture of these focal adhesion proteins was markedly decreased following hyperactivation of the EGF receptor by exogenous EGF. For example in HN5 cells treated with EGF, p130CAS was decreased 21, 49, and 29% after 1, 3, and 15 min, respectively. ARF GTPase-activating protein GIT1 was decreased by EGF treatment 36 and 43% after 3 and 15 min and FAK was decreased 51% after a 1 min (Table IV). A decrease in focal adhesion complex phosphorylation following EGF addition is consistent with data obtained in A431 cells and indicate that despite EGF receptor-mediated phosphorylation of focal adhesion proteins, the phosphotyrosine content of the complex was decreased due to the rapid phosphatase activation and dephosphorylation of focal adhesion complexes (13). Protein complexes were modeled using the pathway analysis Network Explorer software and through literature

data (Fig. 7*A*). Data from ICAT and immunoblot experiments were superimposed upon this framework to visualize points of regulation (Fig. 7*B*).

Interestingly, EGF receptor kinase inhibition for 120 min elicited a similar more modest pattern of decreased recovery of focal adhesion regulating proteins within the phosphotyrosine fraction (Table IV and Fig. 7). For example, erlotinib reduced anti-pY capture of FAK1 by 58%. Similarly, immunoblot experiments indicate p130CAS was reduced in the anti-pY fraction but not in the anti-EGF receptor fraction, consistent with a reduction in tyrosine phosphorylation state but not in EGF receptor interaction (Fig. 7*B*), which was underestimated by ICAT labeling (Table IV). Similarly, anti-pY capture of paxillin, p130CAS, and the FAK homolog Pyk2 were all reduced by EGF receptor inhibition (Fig. 7*B*), while no changes in the phosphorylation of ACK1, α-catenin, or Tyk2 (Figs. 6 and 7*B*) were observed. In HN5 cells, transient EGF receptor inhibition directly or indirectly reduced phosphorylation of cell adhesion components.

DISCUSSION

The sustained activation of the EGF receptor tyrosine kinase, through mutation or autocrine and paracrine stimulation, has been shown to promote phenotypic transformation *in vitro* and *in vivo* (36–38). The biological experiments performed here, in a model of HNSCC, have identified proteins tyrosine-phosphorylated predominantly by EGF receptor and Src family kinases, and proteins that form stable associations with tyrosine-phosphorylated proteins, comprising multiple functional classes (Fig. 3 and Table I). The anti-pY affinity capture method enabled a broad view of EGF receptor and cell adhesion signaling under conditions of EGF receptor autocrine activation, of hyperactivation with exogenous ligand, and of kinase inhibition. Antibody capture methods can suffer from an unacceptable level of nonspecific binding, confounding the identification of proteins specifically interacting with a given target. The use of both an EGF receptor kinase inhibitor and EGF stimulation allowed us to discern pharmacologically and physiologically regulated events, relatively insensitive to the effects of nonspecific binding. We also used several approaches to minimize nonspecific binding, including preabsorption to blank affinity resin, the use of covalently bound pH 3 washed antibody resin, and the use of 0.1% Triton in the initial wash steps. Multiple phosphorylation sites, both novel and known, could be mapped despite the complexity of the peptide mixtures. In proteins showing a sharp treatment-related decrease in anti-pY selection (*e.g.* Erk and Vav-2), the dynamic range of ICAT measurements was sometimes limited by baseline noise within MS spectra. Thus the combined use of the higher-throughput ICAT approach to identify biologically modulated proteins, followed by immunoblotting to verify and more accurately measure protein abundance, was useful. Multiple biological and LC-MS/MS experiments were performed for both protein identification and for ICAT quantitation. The average error in ICAT measurements between repeat experiments (Table IV) was 6%. While the reproducibility in quantitation of peptides between experiments was high, the reproducibility in peptide identification between experiments was considerably more variable. This is likely due to the relatively high degree of sample complexity and the potential for variable ion suppression between LC-MS/MS and biological experiments. Ion suppression effects would likely be improved with additional fractionation by SCX prior LC-MS/MS.

EGF Receptor Immediate Signaling Complexes and Receptor Cross-talk—HN5 cells were shown to utilize multiple SH2 scaffolding proteins NSP1, NSP2, Grb2, Shc, PI3-kinase, PLCγ, STAT3, c-Src, c-Yes, Cbl E3-ligase, Cbl-B, Vav-2, and possibly Tyk2 to establish signaling complexes. NSP1, NSP2 (39), and Vav2 (40, 41) can directly interact with EGF receptors and function as guanine nucleotide exchange factors (GEFs) for small G-proteins of the Ras and Rho family, respectively. Phosphorylation of the mature EGF receptor from HN5 cells was observed on tyrosines Y845, Y992, and Y1068 (by immunoblot) and Y974, Y1086, Y1114, Y1148, and Y1173 (by LC-MS/MS), establishing SH2 and PTB interaction sites. *In vitro* addition of 1 mM ATP and active Src to EGF receptor immunocomplexes identified Y703, Y740 as additional tyrosine phosphorylation sites (data not shown), but it is not known whether such sites can be utilized *in vivo*. However, synthetic phosphopeptide binding studies do highlight Y703, Y740, Y992, and Y1173 as Shc interaction motifs and Y740, Y1068, Y1086, Y114, and Y1148 as Grb2 interactions sites (42).

Complex assembly mediated by SH2 and PTB domain interaction is important not only for the generation of mitogenic and survival signals, but also for the regulation of the rate and route of EGF receptor internalization and consequent signal termination. For example, the SH2 domain-containing E3 ligases, Cbl and Cbl-B, both present within the anti-pY and anti-EGFR fractions, can interact with EGF receptor either directly via SH2 interaction or via SH3 interaction through the SH2-containing adapter Grb2 and are required for efficient proteosomal degradation of the receptor (43–45). Grb2 further interacts with dynamin to promote the transition of internalization complexes from coated pits to endosomal vesicles. Disruption of Cbl function, for example in v-Cbl, transforms cells in part by rerouting activated receptor tyrosine kinases, including EGF receptor, back to the cell surface and promoting their escape from proteosomal degradation. The actions of Cbl receptor degradation are quite specific for the individual erbB family members. EGF receptor homodimers are efficiently down-regulated and degraded in response to Cbl binding, while EGF receptor-ErbB2 heterodimers show a greater degree of recycling back to the cell membrane and thus exhibit enhanced cellular transforming activity (46). The endosomal sorting signal generated by Cbl requires EGF receptor kinase activity (45) and the phosphorylation sites within

the C-terminal tail (47), which may explain the accumulation of total EGF receptor observed after kinase inhibition (Fig. 5).

Members of the Src family of nonreceptor tyrosine kinase have been shown to influence cell proliferation, survival, cell adhesion, and migration, and Src has been shown to cooperate with EGF receptor to enhance cellular transformation, independently of receptor ligand binding (28). Both Src and Yes directly interact with and can be activated by EGF receptor (39), and Src was recently shown to contribute to constitutive phosphorylation and activation of STAT3 in HNSCC cell lines, independently of JAK kinases (48). In HN5 cells, the phosphorylation of EGF receptor on pY845 (49) and the phosphorylation of Src on pY419, a site required for Src kinase activation, indicate Src family kinases were in an active conformation and can contribute to downstream signaling. In contrast to Src and IGF-1 receptor, where phosphorylation of the respective kinase loops is required for full kinase activation, phosphorylation of EGFR Y845 has little effect on kinase activity (50). Recent data suggest Y845 may function as a docking site for downstream effectors (51). Inhibition of EGF receptor kinase activity reduced Src family phosphorylation at Y845, consistent with findings in other cell types (39). At physiological ATP concentrations, this quinazoline class of EGF receptor kinase inhibitor has no detectable direct effect on Src kinase activity (52), indicating Src family activation was in part dependent on EGF receptor kinase activity. While EGF receptor blockade inhibited Src/Yes mediated EGFR Y845 phosphorylation (Fig. 5) and LPA phosphorylation of Erk, Akt and S6 (Fig. 8), the phosphotyrosine Y419 signal from the Src family showed little change for up to 120 min following EGF receptor kinase inhibition. These data suggest that while EGF receptor associated Src family activity may be down-regulated in response to receptor kinase inhibition, while the total pool of Src family activity remained unchanged, suggesting compartmentalization of different Src "pools." Cross-talk between the IGF-1 receptor and EGF receptor also was observed (Fig. 8), where EGFR kinase blockade attenuated the IGF-1 stimulation of Erk and ribosomal S6 phosphorylation (Fig. 8). This is in agreement with data from HB4A cells, where EGF receptor blockade down-regulated IGF-1-stimulated Erk phosphorylation (53). Interestingly, IGF-1 stimulation reduced basal Erk phosphorylation in EGF receptor-overexpressing HN5 cells, suggesting competition between the two receptors for access to components of the Ras-Raf-MEK pathway.

Cell Adhesion Complexes—The control of actin filament formation and cell-cell contacts, associated with cell adhesion, cell migration, and mitosis, are critical to the maintenance of normal cell function. Multiple members of focal adhesion and cell-cell junction complexes were identified by anti-pY and anti-EGFr selection and LC-MS/MS approaches. Of these, FAK, Pyk2, p130CAS, ARF-GIT1, and paxillin were modulated by activation and inhibition of EGF receptor kinase activity. Ligand-activated EGF receptor forms complexes with the C-terminal domain of FAK and Y397 in the N-terminal domain of FAK is phosphorylated upon EGF stimulation. FAK is required for EGF-stimulated cell migration, though its kinase activity is not obligatory (12). Paradoxically, hyperactivation of the EGF receptor by EGF addition lead to a time-dependent decrease in the recovery of p130CAS, Pyk, paxillin, and FAK in the phosphotyrosine affinity fraction (Table IV). However, this may be explained by the reciprocal relationship between EGF receptor activity and focal adhesion formation involving FAK, p130CAS, and paxillin (13). Studies by Lu and coworkers indicate that growth factor receptor activation recruits a tyrosine phosphatase, likely SHP, to dephosphorylate and disrupt focal adhesion complexes, thereby allowing cell migration. When the EGF receptor kinase was transiently inhibited by erlotinib, a similar pattern of focal adhesion phosphoprotein decrease was observed, for example for FAK as measured by ICAT labeling and for Pyk and paxillin by immunoblot (Fig. 7*B*). This also was observed for p130CAS, where isolation within the phosphotyrosine affinity fraction was decreased by EGF receptor blockade (Fig. 7*B*), while interaction with EGF receptor was unchanged. The data indicate transient EGF receptor inhibition also leads to decreased phosphorylation of focal adhesion components, suggesting a close balance between the phosphorylation of focal adhesion components and tyrosine phosphatase activation.

The catenins and plakophilins are members of the armadillo family of proteins and serve in the assembly of cadherin and desmosomal complexes important in cell-cell interaction (54). Tyrosine phosphorylation of β-catenin (Y654) by EGF receptor has been shown to disrupt the complex linking E-cadherin to α-catenin and actin filaments (55–57), and the decreased expression of α-catenin and E-cadherin has been proposed to contribute to the aggressiveness of basaloid squamous carcinoma (58). Following inhibition of EGF receptor kinase activity, the only changes occurring in these complexes were a modest decrease in phosphorylation and/or association of plakophilin. However, the presence of CD98, integrin $\alpha_6\beta_4$, and bullous pemphigoid antigen (BPAG) within the phosphotyrosine fraction was of interest. The cell-surface integrin $\alpha_6\beta_4$ functions as a adhesive receptor for the basement membrane laminins (59) and forms complex(s) with BPAG, plectin, and keratin filaments, which are dissolved by EGF receptor activation to allow migration (60). CD98 has been reported to be constitutively associated with integrin and functions to cluster and activate integrins resulting in PI3-kinase and Akt activation and anchorage-independent growth (61). While activation of integrin-linked kinase (ILK) can lead to tyrosine phosphorylation of integrin β_4 and subsequent activation of Erk and PI3-kinase mitogenic and survival signaling pathways, both integrin $\alpha_6\beta_4$ and EGF receptor have been shown to directly associate, also promoting integrin β_4 phosphorylation possibly through associated Src family kinases Fyn and Yes. Conversely, integrin receptor complexes can activate EGF receptor in a Src- and p130CAS-dependent manner, leading to EGF receptor phosphorylation at Y845, Y1068, Y1086, and Y1173

(62). While no modulation of integrin or CD98 by EGF or erlotinib was observed, it is formally possible for these complexes to use EGF receptor as a signaling scaffold in a receptor kinase-independent manner. These data suggest additional mechanisms by EGF receptor might serve as a signaling scaffold independent of its kinase activity.

Rapid methods for identifying EGF receptor-associated pathway constituents and semi-quantitatively assess the impact of EGF receptor kinase activity on protein phosphorylation and complex formation were established. Proteins and complexes with known and poorly described functions were unequivocally identified by anti-pY and anti-EGFR affinity selection and pathways modeled. Specific interactions between EGF receptor, adaptor proteins, downstream signaling components, and interacting kinases were observed that could be modulated by EGF receptor kinase activity. Protein interactions within these complexes can be further refined by specific antibody selection experiments or by tandem affinity selection by expression of epitope-tagged cDNAs (63, 64). While the activation of TCF-LEF, STAT3/5, and AP-1 are relatively well studied, the role for EGF receptor kinase as a nuclear factor directly contributing to transcription has only recently been documented (65, 66). The recovery of nuclear transport and transcription components, though suggestive of a direct role for the EGF receptor kinase in transcription, also may be explained by nuclear localization of phosphorylated STAT3 and its known association tranporter protein importin-β1 (67). Functional interactions between EGF receptor, IGF-1 receptor, Src, and LPA signaling converged in downstream Mek-Erk and PI-3 kinase pathways and suggest EGF receptor can additionally serve as a ligand-independent signaling scaffold for distinct kinases. The recent development of methods for multiplex isobaric peptide labeling provide increased sensitivity and dynamic range, enabling time and dose studies in sensitive and resistant tumor lines and xenografts (68). The application of these methods to the further examination of EGF receptor and cell adhesion signaling will allow time-dependent quantitation of phosphotyrosine-containing proteins complexes following kinase activation and inhibition between tumor cells responsive and insensitive to EGF receptor blockade.

Acknowledgments—We thank Heng Pan for technical assistance, Sally Webb and Lydia Nuwaysir for assistance with ProID, ProICAT and CeleraCDS search and database programs, and Arthur Bruskin for critical discussion.

* The costs of publication of this article were defrayed in part by the payment of page charges. This article must therefore be hereby marked "*advertisement*" in accordance with 18 U.S.C. Section 1734 solely to indicate this fact.

S The on-line version of this manuscript (available at http://www.mcponline.org) contains supplemental material.

‡‡ Current address: Amersham Bioscience, Piscattaway, NJ.

§§ To whom correspondence should be addressed: OSI Pharmaceuticals, Inc., 1 Bioscience Park Drive, Farmingdale, NY 11735. Tel.: 631-962-0709; Fax: 631-845-5671; E-mail: jhaley@osip.com.

REFERENCES

1. Yarden, Y. (2001) The EGFR family and its ligands in human cancer. Signalling mechanisms and therapeutic opportunities. *Eur. J. Cancer* **37,** Suppl 4, S3–S8
2. Prenzel, N., Zwick, E., Leserer, M., and Ullrich, A. (2000) Tyrosine kinase signalling in breast cancer. Epidermal growth factor receptor: Convergence point for signal integration and diversification. *Breast Cancer Res.* **2,** 184–190
3. Nicholson, R. I., Gee, J. M., and Harper, M. E. (2001) EGFR and cancer prognosis. *Eur. J. Cancer* **37,** Suppl 4, S9–S15
4. Yarden, Y., and Sliwkowski, M. X. (2001) Untangling the ErbB signalling network. *Nat. Rev. Mol. Cell. Biol.* **2,** 127–137
5. Downward, J., Yarden, Y., Mayes, E., Scrace, G., Totty, N., Stockwell, P., Ullrich, A., Schlessinger, J., and Waterfield, M. D. (1984) Close similarity of epidermal growth factor receptor and v-erb-B oncogene protein sequences. *Nature* **307,** 521–527
6. Schlessinger, J. (2002) Ligand-induced, receptor-mediated dimerization and activation of EGF receptor. *Cell* **110,** 669–672
7. Pawson, T., and Nash, P. (2003) Assembly of cell regulatory systems through protein interaction domains. *Science* **300,** 445–452
8. Carpenter, G. (2000) The EGF receptor: A nexus for trafficking and signaling. *Bioessays* **22,** 697–707
9. Vivanco, I., and Sawyers, C. L. (2002) The phosphatidylinositol 3-kinase AKT pathway in human cancer. *Nat. Rev. Cancer* **2,** 489–501
10. Dancey, J. E. (2004) Predictive factors for epidermal growth factor receptor inhibitors—The bull's-eye hits the arrow. *Cancer Cell* **5,** 411–415
11. Comoglio, P. M., Boccaccio, C., and Trusolino, L. (2003) Interactions between growth factor receptors and adhesion molecules: Breaking the rules. *Curr. Opin. Cell Biol.* **15,** 565–571
12. Sieg, D. J., Hauck, C. R., Ilic, D., Klingbeil, C. K., Schaefer, E., Damsky, C. H., and Schlaepfer, D. D. (2000) FAK integrates growth-factor and integrin signals to promote cell migration. *Nat. Cell Biol.* **2,** 249–256
13. Lu, Z., Jiang, G., Blume-Jensen, P., and Hunter, T. (2001) Epidermal growth factor-induced tumor cell invasion and metastasis initiated by dephosphorylation and downregulation of focal adhesion kinase. *Mol. Cell. Biol.* **21,** 4016–4031
14. Knight, J., Gusterson, B. A., Cowley, G., and Monaghan, P. (1984) Differentiation of normal and malignant human squamous epithelium *in vivo* and *in vitro*: A morphologic study. *Ultrastruct. Pathol.* **7,** 133–141
15. Pollack, V. A., Savage, D. M., Baker, D. A., Tsaparikos, K. E., Sloan, D. E., Moyer, J. D., Barbacci, E. G., Pustilnik, L. R., Smolarek, T. A., Davis, J. A., Vaidya, M. P., Arnold, L. D., Doty, J. L., Iwata, K. K., and Morin, M. J. (1999) Inhibition of epidermal growth factor receptor-associated tyrosine phosphorylation in human carcinomas with CP-358,774: Dynamics of receptor inhibition in situ and antitumor effects in athymic mice. *J. Pharmacol. Exp. Ther.* **291,** 739–748
16. Moyer, J. D., Barbacci, E. G., Iwata, K. K., Arnold, L., Boman, B., Cunningham, A., DiOrio, C., Doty, J., Morin, M. J., Moyer, M. P., Neveu, M., Pollack, V. A., Pustilnik, L. R., Reynolds, M. M., Sloan, D., Theleman, A., and Miller, P. (1997) Induction of apoptosis and cell cycle arrest by CP-358,774, an inhibitor of epidermal growth factor receptor tyrosine kinase. *Cancer Res.* **57,** 4838–4848
17. Gygi, S. P., Rist, B., Gerber, S. A., Turecek, F., Gelb, M. H., and Aebersold, R. (1999) Quantitative analysis of complex protein mixtures using isotope-coded affinity tags. *Nat. Biotechnol.* **17,** 994–999
18. Waterfield, M. D., Mayes, E. L., Stroobant, P., Bennet, P. L., Young, S., Goodfellow, P. N., Banting, G. S., and Ozanne, B. (1982) A monoclonal antibody to the human epidermal growth factor receptor. *J. Cell. Biochem.* **20,** 149–161
19. Wolters, D. A., Washburn, M. P., and Yates, J. R., 3rd (2001) An automated multidimensional protein identification technology for shotgun proteomics. *Anal. Chem.* **73,** 5683–5690
20. Kwok, T. T., and Sutherland, R. M. (1991) Differences in EGF related radiosensitisation of human squamous carcinoma cells with high and low numbers of EGF receptors. *Br. J. Cancer* **64,** 251–254
21. Downward, J., Parker, P., and Waterfield, M. D. (1984) Autophosphorylation sites on the epidermal growth factor receptor. *Nature* **311,** 483–485
22. Margolis, B. L., Lax, I., Kris, R., Dombalagian, M., Honegger, A. M., Howk, R., Givol, D., Ullrich, A., and Schlessinger, J. (1989) All autophosphorylation sites of epidermal growth factor (EGF) receptor and HER2/neu are

located in their carboxyl-terminal tails. Identification of a novel site in EGF receptor. *J. Biol. Chem.* **264,** 10667–10671
23. Haugh, J. M., and Meyer, T. (2002) Active EGF receptors have limited access to PtdIns(4,5)P(2) in endosomes: Implications for phospholipase C and PI 3-kinase signaling. *J. Cell Sci.* **115,** 303–310
24. Blagoev, B., Kratchmarova, I., Ong, S. E., Nielsen, M., Foster, L. J., and Mann, M. (2003) A proteomics strategy to elucidate functional protein-protein interactions applied to EGF signaling. *Nat. Biotechnol.* **21,** 315–318
25. Steen, H., Kuster, B., Fernandez, M., Pandey, A., and Mann, M. (2002) Tyrosine phosphorylation mapping of the epidermal growth factor receptor signaling pathway. *J. Biol. Chem.* **277,** 1031–1039
26. Lim, Y. P., Diong, L. S., Qi, R., Druker, B. J., and Epstein, R. J. (2003) Phosphoproteomic fingerprinting of epidermal growth factor signaling and anticancer drug action in human tumor cells. *Mol. Cancer Ther.* **2,** 1369–1377
27. Mann, M., Ong, S. E., Gronborg, M., Steen, H., Jensen, O. N., and Pandey, A. (2002) Analysis of protein phosphorylation using mass spectrometry: Deciphering the phosphoproteome. *Trends Biotechnol.* **20,** 261–268
28. Tice, D. A., Biscardi, J. S., Nickles, A. L., and Parsons, S. J. (1999) Mechanism of biological synergy between cellular Src and epidermal growth factor receptor. *Proc. Natl. Acad. Sci. U. S. A.* **96,** 1415–1420
29. Daub, H., Wallasch, C., Lankenau, A., Herrlich, A., and Ullrich, A. (1997) Signal characteristics of G protein-transactivated EGF receptor. *EMBO J.* **16,** 7032–7044
30. Wu, J., and Cunnick, J. M. (2002) Trans-regulation of epidermal growth factor receptor by lysophosphatidic acid and G protein-coupled receptors. *Biochim. Biophys. Acta* **1582,** 100–106
31. Cunnick, J. M., Dorsey, J. F., Standley, T., Turkson, J., Kraker, A. J., Fry, D. W., Jove, R., and Wu, J. (1998) Role of tyrosine kinase activity of epidermal growth factor receptor in the lysophosphatidic acid-stimulated mitogen-activated protein kinase pathway. *J. Biol. Chem.* **273,** 14468–14475
32. Wasilenko, W. J., Payne, D. M., Fitzgerald, D. L., and Weber, M. J. (1991) Phosphorylation and activation of epidermal growth factor receptors in cells transformed by the src oncogene. *Mol. Cell. Biol.* **11,** 309–321
33. Maa, M. C., Leu, T. H., McCarley, D. J., Schatzman, R. C., and Parsons, S. J. (1995) Potentiation of epidermal growth factor receptor-mediated oncogenesis by c-Src: Implications for the etiology of multiple human cancers. *Proc. Natl. Acad. Sci. U. S. A.* **92,** 6981–6985
34. Hanks, S. K., Ryzhova, L., Shin, N. Y., and Brabek, J. (2003) Focal adhesion kinase signaling activities and their implications in the control of cell survival and motility. *Front. Biosci.* **8,** d982–996
35. Goldberg, G. S., Alexander, D. B., Pellicena, P., Zhang, Z. Y., Tsuda, H., and Miller, W. T. (2003). Src phosphorylates Cas on tyrosine 253 to promote migration of transformed cells. *J. Biol. Chem.* **278,** 46533–46540
36. Mendelsohn, J., and Baselga, J. (2003) Status of epidermal growth factor receptor antagonists in the biology and treatment of cancer. *J. Clin. Oncol.* **21,** 2787–2799
37. Velu, T. J., Beguinot, L., Vass, W. C., Willingham, M. C., Merlino, G. T., Pastan, I., and Lowy, D. R. (1987) Epidermal-growth-factor-dependent transformation by a human EGF receptor proto-oncogene. *Science* **238,** 1408–1410
38. Di Fiore, P. P., Pierce, J. H., Fleming, T. P., Hazan, R., Ullrich, A., King, C. R., Schlessinger, J., and Aaronson, S. A. (1987) Overexpression of the human EGF receptor confers an EGF-dependent transformed phenotype to NIH 3T3 cells. *Cell* **51,** 1063–1070
39. Osherov, N., and Levitzki, A. (1994) Epidermal-growth-factor-dependent activation of the src-family kinases. *Eur. J. Biochem.* **225,** 1047–1053
40. Pandey, A., Podtelejnikov, A. V., Blagoev, B., Bustelo, X. R., Mann, M., and Lodish, H. F. (2000) Analysis of receptor signaling pathways by mass spectrometry: Identification of vav-2 as a substrate of the epidermal and platelet-derived growth factor receptors. *Proc. Natl. Acad. Sci. U. S. A.* **97,** 179–184
41. Tamas, P., Solti, Z., Bauer, P., Illes, A., Sipeki, S., Bauer, A., Farago, A., Downward, J., and Buday, L. (2003) Mechanism of epidermal growth factor regulation of Vav2, a guanine nucleotide exchange factor for Rac. *J. Biol. Chem.* **278,** 5163–5171
42. Ward, C. W., Gough, K. H., Rashke, M., Wan, S. S., Tribbick, G., and Wang, J. (1996) Systematic mapping of potential binding sites for Shc and Grb2 SH2 domains on insulin receptor substrate-1 and the receptors for insulin, epidermal growth factor, platelet-derived growth factor, and fibroblast growth factor. *J. Biol. Chem.* **271,** 5603–5609
43. Galisteo, M. L., Dikic, I., Batzer, A. G., Langdon, W. Y., and Schlessinger, J. (1995) Tyrosine phosphorylation of the c-cbl proto-oncogene protein product and association with epidermal growth factor (EGF) receptor upon EGF stimulation. *J. Biol. Chem.* **270,** 20242–20245
44. Meisner, H., and Czech, M. P. (1995) Coupling of the proto-oncogene product c-Cbl to the epidermal growth factor receptor. *J. Biol. Chem.* **270,** 25332–25335
45. Levkowitz, G., Waterman, H., Zamir, E., Kam, Z., Oved, S., Langdon, W. Y., Beguinot, L., Geiger, B., and Yarden, Y. (1998) c-Cbl/Sli-1 regulates endocytic sorting and ubiquitination of the epidermal growth factor receptor. *Genes Dev.* **12,** 3663–3674
46. Muthuswamy, S. K., Gilman, M., and Brugge, J. S. (1999) Controlled dimerization of ErbB receptors provides evidence for differential signaling by homo- and heterodimers. *Mol. Cell. Biol.* **19,** 6845–6857
47. Sorkin, A., Helin, K., Waters, C. M., Carpenter, G., and Beguinot, L. (1992) Multiple autophosphorylation sites of the epidermal growth factor receptor are essential for receptor kinase activity and internalization. Contrasting significance of tyrosine 992 in the native and truncated receptors. *J. Biol. Chem.* **267,** 8672–8678
48. Xi, S., Zhang, Q., Dyer, K. F., Lerner, E. C., Smithgall, T. E., Gooding, W. E., Kamens, J., and Grandis, J. R. (2003) Src kinases mediate STAT growth pathways in squamous cell carcinoma of the head and neck. *J. Biol. Chem.* **278,** 31574–31583
49. Biscardi, J. S., Ishizawar, R. C., Silva, C. M., and Parsons, S. J. (2000) Tyrosine kinase signalling in breast cancer: Epidermal growth factor receptor and c-Src interactions in breast cancer. *Breast Cancer Res.* **2,** 203–210
50. Gotoh, N., Tojo, A., Hino, M., Yazaki, Y., and Shibuya, M. (1992) A highly conserved tyrosine residue at codon 845 within the kinase domain is not required for the transforming activity of human epidermal growth factor receptor. *Biochem. Biophys. Res. Commun.* **186,** 768–774
51. Boerner, J. L., Demory, M. L., Silva, C., and Parsons, S. J. (2004) Phosphorylation of Y845 on the epidermal growth factor receptor mediates binding to the mitochondrial protein cytochrome c oxidase subunit II. *Mol. Cell. Biol.* **24,** 7059–7071
52. Kitagawa, D., Tanemura, S., Ohata, S., Shimizu, N., Seo, J., Nishitai, G., Watanabe, T., Nakagawa, K., Kishimoto, H., Wada, T., Tezuka, T., Yamamoto, T., Nishina, H., and Katada, T. (2002) Activation of extracellular signal-regulated kinase by ultraviolet is mediated through Src-dependent epidermal growth factor receptor phosphorylation. Its implication in an anti-apoptotic function. *J. Biol. Chem.* **277,** 366–371
53. Ahmad, T., Farnie, G., Bundred, N. J., and Anderson, N. G. (2004) The mitogenic action of insulin-like growth factor I in normal human mammary epithelial cells requires the epidermal growth factor receptor tyrosine kinase. *J. Biol. Chem.* **279,** 1713–1719
54. Hofmann, I., Mertens, C., Brettel, M., Nimmrich, V., Schnolzer, M., and Herrmann, H. (2000) Interaction of plakophilins with desmoplakin and intermediate filament proteins: An *in vitro* analysis. *J. Cell Sci.* **113,** 2471–2483
55. Hoschuetzky, H., Aberle, H., and Kemler, R. (1994) Beta-catenin mediates the interaction of the cadherin-catenin complex with epidermal growth factor receptor. *J. Cell Biol.* **127,** 1375–1380
56. Bonvini, P., An, W. G., Rosolen, A., Nguyen, P., Trepel, J., Garcia de Herreros, A., Dunach, M., and Neckers, L. M. (2001) Geldanamycin abrogates ErbB2 association with proteasome-resistant β-catenin in melanoma cells, increases β-catenin-E-cadherin association, and decreases β-catenin-sensitive transcription. *Cancer Res.* **61,** 1671–1677
57. Hu, P., O'Keefe, E. J., and Rubenstein, D. S. (2001) Tyrosine phosphorylation of human keratinocyte β-catenin and plakoglobin reversibly regulates their binding to E-cadherin and α-catenin. *J. Invest. Dermatol.* **117,** 1059–1067
58. Tsubochi, H., Suzuki, T., Suzuki, S., Ohashi, Y., Ishibashi, S., Moriya, T., Fujimura, S., and Sasano, H. (2000) Immunohistochemical study of basaloid squamous cell carcinoma, adenoid cystic and mucoepidermoid carcinoma in the upper aerodigestive tract. *Anticancer Res.* **20,** 1205–1211
59. Mercurio, A. M., Rabinovitz, I., and Shaw, L. M. (2001) The $\alpha_6\beta_4$ integrin and epithelial cell migration. *Curr. Opin. Cell Biol.* **13,** 541–545
60. Mariotti, A., Kedeshian, P. A., Dans, M., Curatola, A. M., Gagnoux-Palacios,

L., and Giancotti, F. G. (2001) EGF-R signaling through Fyn kinase disrupts the function of integrin $\alpha_6\beta_4$ at hemidesmosomes: Role in epithelial cell migration and carcinoma invasion. *J. Cell Biol.* **155,** 447–458
61. Rintoul, R. C., Buttery, R. C., Mackinnon, A. C., Wong, W. S., Mosher, D., Haslett, C., and Sethi, T. (2002) Cross-linking CD98 promotes integrin-like signaling and anchorage-independent growth. *Mol. Biol. Cell* **13,** 2841–2852
62. Moro, L., Dolce, L., Cabodi, S., Bergatto, E., Erba, E. B., Smeriglio, M., Turco, E., Retta, S. F., Giuffrida, M. G., Venturino, M., Godovac-Zimmermann, J., Conti, A., Schaefer, E., Beguinot, L., Tacchetti, C., Gaggini, P., Silengo, L., Tarone, G., and Defilippi, P. (2002) Integrin-induced epidermal growth factor (EGF) receptor activation requires c-Src and p130CAS and leads to phosphorylation of specific EGF receptor tyrosines. *J. Biol. Chem.* **277,** 9405–9414
63. Graumann, J., Dunipace, L. A., Seol, J. H., McDonald, W. H., Yates, J. R., 3rd, Wold, B. J., and Deshaies, R. J. (2004) Applicability of tandem affinity purification MudPIT to pathway proteomics in yeast. *Mol. Cell. Proteomics* **3,** 226–237
64. Rigaut, G., Shevchenko, A., Rutz, B., Wilm, M., Mann, M., and Seraphin, B. (1999) A generic protein purification method for protein complex characterization and proteome exploration. *Nat. Biotechnol.* **17,** 1030–1032
65. Lin, S. Y., Makino, K., Xia, W., Matin, A., Wen, Y., Kwong, K. Y., Bourguignon, L., and Hung, M. C. (2001) Nuclear localization of EGF receptor and its potential new role as a transcription factor. *Nat. Cell Biol.* **3,** 802–808
66. Waugh, M. G., and Hsuan, J. J. (2001) EGF receptors as transcription factors: Ridiculous or sublime? *Nat. Cell Biol.* **3,** E209–E211
67. Fagerlund, R., Melen, K., Kinnunen, L., and Julkunen, I. (2002) Arginine/lysine-rich nuclear localization signals mediate interactions between dimeric STATs and importin α5. *J. Biol. Chem.* **277,** 30072–30078
68. Haley, J. D., Petti, F., Theleman, A., Pappin, D. J., Purkayastha, S., and Zieske, L. (2004). A novel fragment ion tag approach to the measurement of tyrosine kinase signaling pathways. *Am. Soc. Mass. Spectr. 52nd Confr.* (abstr. 386)